Bulletin of Earthquake Engineering (2019) 17:3895–3932
https://doi.org/10.1007/s10518-019-00638-9

ORIGINAL RESEARCH

Haunch retrofitting technique for seismic upgrading deficient RC frames

Naveed Ahmad[1] · Junaid Akbar[1] · Muhammad Rizwan[1] · Bashir Alam[1] · Akhtar Naeem Khan[1] · Abdul Lateef[1]

Received: 10 April 2018 / Accepted: 9 May 2019 / Published online: 14 May 2019

Abstract
Haunch retrofitting technique has been employed, primarily to stiffen the beam-column connections that controls the hierarchy of strength within the beam-column members, and avoid joint shear hinging of RC frame structures, subjected to earthquake imposed lateral loads. Shake-table tests were performed on a total of nine (09) 1:3 reduced scale two-story RC frames, including five (05) as-built and four (04) haunch retrofitted models, to develop structures' damage scale and obtain their seismic response parameters. A representative finite element based numerical model was prepared in SeismoStruct and validated against the experimental response. A suit of seven natural accelerograms were retrieved from the PEER NGA strong ground motions database and employed for incremental dynamic analysis of structural models, in order to derive seismic fragility functions for as-built and retrofitted structures. Vulnerability curves were derived for the structures, correlating the mean damage ratio with the seismic intensity. Uniform hazard curves, obtained for candidate cities in moderate and high hazard zones, were employed to derive the structures' loss exceedance curves for calculating the expected average annual loss. The net present value of the annual avoided repair cost was quantified, and critically compared with the retrofitting cost, to evaluate the viability of haunch retrofitting technique for seismic upgradation of deficient RC frame structures for risk mitigation.

Keywords Strengthening · Steel haunch · Retrofitting · Cost-benefit analysis · Risk mitigation · Seismic upgrading

1 Introduction

Earthquake observations, in many developing countries during recent past events, have revealed the high seismic vulnerability of deficient reinforced concrete frame structures. This is primarily due to the construction defects inherently found in these structures, consequently resulting into enormous loss of lives and economic losses (Arslan and Korkmaz 2007; Ates et al. 2013; Bal et al. 2008; Bothara and Hicyilmas 2008; Chaulagain et al.

✉ Naveed Ahmad
naveed.ahmad@uetpeshawar.edu.pk

1 Earthquake Engineering Center, UET Peshawar, Peshawar, Khyber Pakhtunkhwa, Pakistan

2015; Doocy et al. 2013; Erdil 2016; Fintel 1995; Ruiz-Pinilla et al. 2016). As observed in earthquakes, and demonstrated through laboratory experiments, substandard materials (low strength concrete, reduced size and low quality re-bars), reduction in longitudinal and transverse reinforcement, inadequate anchorage of longitudinal beam reinforcement in joints and joints lacking confining ties are major factors making structure incapable of withstanding moderate-to-strong earthquake shaking, which lead to damage and early collapse of frame buildings during earthquakes (Ahmad et al. 2019; Aycardi et al. 1994; Badrashi et al. 2010; Beres et al. 1996; Bracci et al. 1995a; Calvi et al. 2002; Fintel 1995; Hakuto et al. 2000; Kuang and Wong 2006; Park 2002; Rizwan et al. 2018; Sharma et al. 2011; Yavari et al. 2013). Various, more or less costly, techniques have been proposed and experimentally validated for the seismic upgradation of deficient RC frame structures (Benavent-Climent et al. 2014; Bracci et al. 1995b; Dolce et al. 2005, 2007; Fintel 1995; Garcia et al. 2010; Ghobarah and Said 2001; Shiravand et al. 2017). Earthquake induced damages in structure if took place in the beam-column joint panels, brittle shear failure mechanism joint shear hinge form at the local level that consequently result in story mechanism at the global level due to columns hinging (Fig. 1). Haunch retrofitting technique was proposed to enhance the seismic performance of RC frames having weaker beam-column joints, where application of other conventional techniques become cumbersome and costly.

Joint panels in real structures are difficult to strengthen with the commonly adopted techniques (Engindeniz et al. 2005), and require application of an intervention that reduce shear demand on joint panels, and instead, allow beam-column members to deform inelastically under earthquake loads. To control the hierarchy of strength within the beam-column members, haunch technique was proposed for RC frames by Pampanin et al. (2006), installing a metallic haunch type element at the beam-column connections of frames, particularly, those experiencing joint shear hinging under lateral loads. A stiffer haunch to remain elastic during loading or deformable (inelastically), to yield during loading and provide supplemental energy dissipation under cyclic response, envisaged to avoid joint damage and enhance seismic performance of structure, as validated experimentally and numerically on 2D beam-column sub-assemblages and frame (Appa-Rao et al. 2013; Genesio 2012; Pampanin et al. 2006; Sharma et al. 2011, 2014; Wang et al. 2017).

However, most of these investigations were limited to the seismic performance assessment of beam-column sub-assemblages under imposed quasi-static cyclic displacement, and experimental/numerical seismic analysis of RC frames against design based

Fig. 1 Joint damageability and, consequent, collapse of structures: from left to right: 1999 Izmit earthquake in Turkey, 1999 Chi-Chi earthquake in Taiwan and 1994 Northridge earthquake in USA (Sharma 2013)

earthquakes. Since, haunch intervention primarily alters the mechanism from brittle joint shear hinging to beam-column members' yielding, at the shifted plastic hinge location, it is the later that governs the seismic resistance and demonstrates the structure's deformability (ductility). Depending on the relative strength of beam-column members, the intended plastic hinge may form desirably in beams, in case of strong-column and weak-beam condition, but otherwise may form inevitably in columns that could lead to unfavorable soft-story global mechanism. For this reason, it is utmost important to evaluate the efficiency of haunch retrofitting technique for both seismically designed structures, but having weaker beam-column joint panels due to lack of confining ties or employing low strength concrete, and structures designed for gravity loads only. Further, the seismic assessment should also consider the economic viability of strengthening technique in both moderate and high seismic hazard regions. It is due to these reasons, cost-benefit analysis of retrofitting interventions getting more attention in recent days, to quantify the economic benefit gained over the retrofit cost for selection of appropriate strengthening schemes (Banazadeh et al. 2017; Cardone et al. 2018; Dyanati et al. 2017; Marques et al. 2018).

For seismic evaluation, a total of nine shake-table tests were conducted on 1:3 reduced scale two-story RC frame structures at the Earthquake Engineering Center of UET Peshawar, under the research program led by the first author for seismic vulnerability assessment and strengthening of deficient modern RC frames in Pakistan, including as-built and haunch retrofitted models. Using natural accelerogram of 1994 Northridge earthquake, incremental multi-levels excitations' tests were performed on models; deforming structure from elastic-to-inelastic and incipient collapse state. Seismic behavior of the models was observed, and damage scale of the respective models was developed. A finite element based numerical model, prepared in SeismoStruct, was calibrated with the experimental observations and employed for incremental dynamic analysis. Using a probabilistic nonlinear dynamic reliability based method (Ahmad et al. 2014), fragility functions were derived for both the as-built and haunch retrofitted models. The structures' fragility functions were transformed to the vulnerability curves, correlating the mean damage ratio of the structure with the seismic intensity. To characterize the seismic hazard of candidate cities, uniform hazard curves were obtained, and employed to develop the structures' loss exceedance curves, which were analyzed to calculate the average annual loss (AAL). The AAL obtained for both the as-built and retrofitted structure models were incorporated in the cost-benefit model to assess the economic viability of haunch retrofitting technique, in both the moderate and high seismic hazard regions.

2 Description of RC frame structures

2.1 As-built RC frame models

The present research considered low-rise reinforced concrete special moment resisting frame (SMRF) structures. In particular a two-story frame normally practiced for low-rise public buildings like hospitals, schools, apartment buildings and shopping malls. It has a regular rectangular plan of 2-bays by 1-bay with center-to-center length of 18 feet (5487 mm) and story height of 12 feet (3658 mm). The considered frame was designed using the lateral static force-based seismic design procedure given in the BCP-SP (2007), which is primarily based on the UBC-97. The structure design was carried out for the high seismic hazard (Zone 4, 0.40 g design PGA on soil type B, as per the NEHRP classification), which was detailed as per the ACI-318-05 recommendations for SMRF. The structure loading included self-weight for structural beam-column members and floor and roof slab, superimposed dead load for floor finishes and loads for partitions/contents: 40 psf (1.915 kN/m^2) on the first floor and 60 psf (2.873 kN/m^2) on the roof, and live load of 60 psf (2.873 kN/m^2) on the first floor and 40 psf (1.915 kN/m^2) on the roof. Concrete with compressive strength of 3000 psi (21 MPa) and reinforcing steel bars with yield strength of 60,000 psi (414 MPa) were considered. The structure design was carried out in the finite element based software CSI ETABS, considering all the load combinations for dead, live and earthquake loads given in the BCP-SP (2007). Figure 2 shows the typical geometric and reinforcement details of the code-conforming frame, extracted from the public type structure (Ahmad et al. 2019), while Table 1 reports details of all the five as-built models (a code-conforming and four deficient models) considered in the present research for assessment.

Recent field surveys carried out in developing countries (Badrashi et al. 2010) have found number of construction defects in the existing building stock. This included the use of substandard construction materials (e.g. low strength concrete and under-sized re-bars), reduced longitudinal and transverse reinforcement in beam-column members, absence of confining ties in beam-column joint panels, using insufficient lap-splice length in plastic hinge region and not practicing 135° standard seismic hooks for transverse ties, among others.

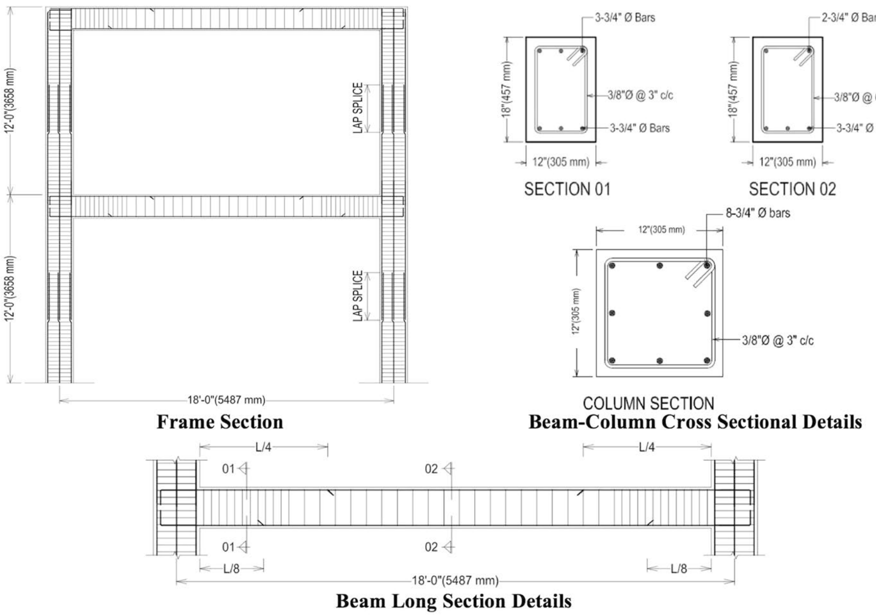

Fig. 2 Typical details of the code-conforming RC frame structure, SMRF detailings

Table 1 Characteristics of as-built frames (disparities in comparison to code-conforming model are highlighted)

<table>
<tr><th>S. No.</th><th>Dimensions in (mm)</th><th>f_c'</th><th>f_y</th><th>Long. Reinf.</th><th>Tran. Reinf.</th><th>Joint Ties</th><th>Hook</th></tr>
<tr><td>Model-1</td><td rowspan="5">Beam: 12 x 18 (30 x 459)
Columns: 12 x 12 (304 x 304)</td><td>3000 psi (21 MPa)</td><td rowspan="5">60 ksi (414 MPa)</td><td rowspan="4">Beam: 6#6 (6ϕ20 mm)
Column: 8#6 (8ϕ20 mm)</td><td rowspan="3">Beam: #3@ 3in (ϕ10mm @ 76mm)
Column: #3@ 3in (ϕ10mm @ 76mm)</td><td rowspan="2">With Ties</td><td rowspan="4">135^0</td></tr>
<tr><td>Model-2</td><td rowspan="4">2000 psi (14 MPa)</td></tr>
<tr><td>Model-3</td><td rowspan="3">No - Ties</td></tr>
<tr><td>Model-4</td><td>Beam: #3@ 6in (ϕ10mm @ 152mm)
Column: #3@ 6in (ϕ10mm @ 152mm)</td></tr>
<tr><td>Model-5</td><td>Beam: 4#6 (4ϕ20 mm)
Column: 6#6 (6ϕ20 mm)</td><td>Beam: #3@ 9in (ϕ10mm @ 228mm)
Column: #3@ 9in (ϕ10mm @ 228mm)</td><td>90^0</td></tr>
</table>

Model-1 is a code conforming model

Model-2 is similar to Model-1, however, concrete strength of this model is 2000 psi (14 MPa)

Model-3 is similar to Model-2, however, ties are not provided in beam-column joint panels

Model-4 is similar to Model-3, however, stirrups in beam and column members are provided with spacing two-times of the code specified

Model-5 is similar to Model-3, however, stirrups in beam and column members are provided with spacing three-times of the code specified

2.2 Design of haunch retrofitting for RC frame

Avoiding joint shear hinging will require an intervention that reduces the moment demand in beam at the beam-column interface, this led to the development of haunch retrofitting technique for RC frames (Pampanin et al. 2006). The application of haunch at the beam-column connection result into opposing localized shear and bending in beam-column members at the point of haunch application, consequently lowering shear and moment demand in beam-column members at the joint interface, thus, reducing shear demand in joint panel zone (Figs. 3, 4).

Depending on the haunch axial stiffness, angle and position of application, the formation of plastic hinge can be enforced in beam to ensure desirable beam-sway mechanism of connection besides avoiding joint shear hinging under lateral loads. Additional less desirable mechanisms like flexure hinging of columns and undesirable mechanism like shear failure of beam and column members, if inevitable in deficient RC frames, may be prioritized, as; beam yielding, column yielding, joint shear hinging, shear failure of beam, shear failure of column, for optimum performance.

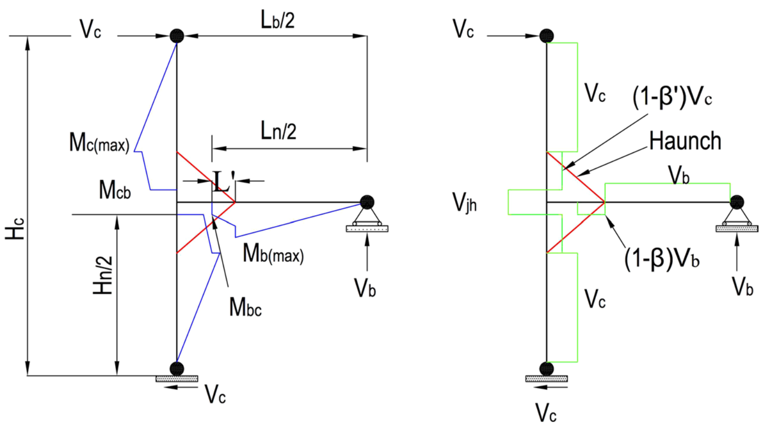

Fig. 3 Modified bending moment and shear actions on haunch retrofitted beam-column sub-assemblages under lateral load

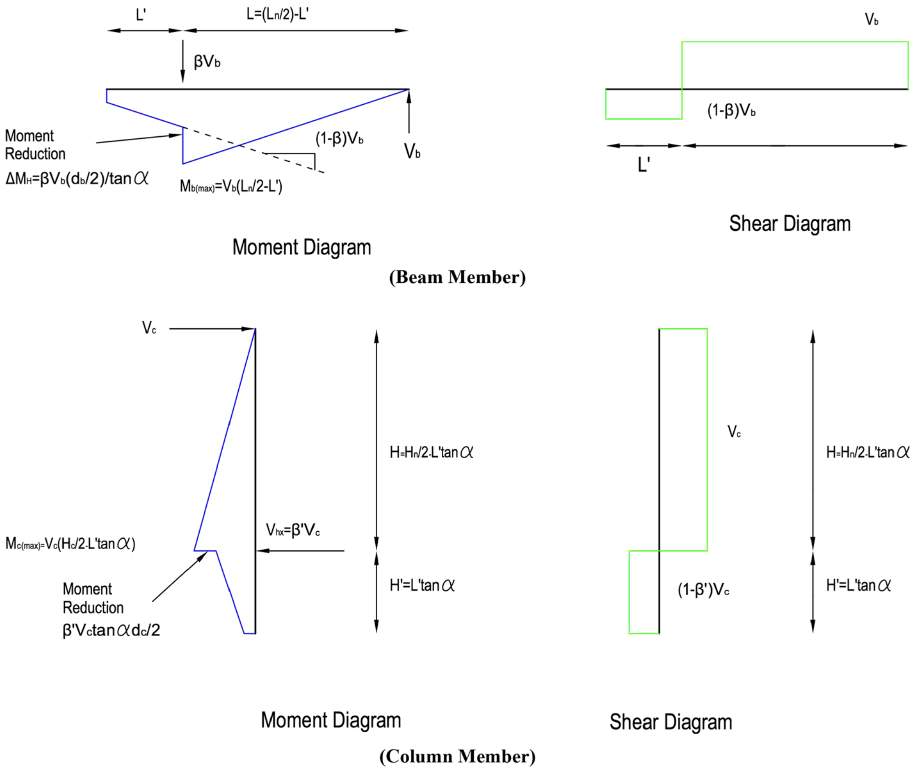

Fig. 4 Moment and shear developed in beam and column members after haunch installation. In this figure, α is angle the haunch makes with the column and d_b is the beam depth

To design haunch retrofit scheme for the considered structures, listed in Table 1, Model 3 and Model 5 were selected, which represents the most commonly found recent constructions (Model-3) and existing structures (Model-5). Moment curvature analysis of beam and column was carried out to compute the yield moment capacity of the members. Considering an optimum value of β equal to 2.5, the minimum required length for haunch application is decided to achieve plastic hinging in beam. For a specified axial stiffness of the haunch element, the value of β can be calculated approximately using analytical formulae (Pampanin et al. 2006) or may be obtained through numerical analysis. Seismic design for the dissipating haunch requires a yieldable element, selected carefully to ensure altering damage mechanism from joint shear hinging to haunch element axial yielding and beam-column members flexure yielding. The most favorable will be to allow yielding in the beam member first, followed by haunch element yielding. Since, there is always a provision in beam moment increase beyond yield due to material overstrength, the designed haunch, corresponding to the yield moment in beam, will develop its yield strength to deform inelastically and dissipate energy through hysteretic response. The dissipating haunch will be subjected to alternate tension and compression, whereby the haunch element will undergo buckling, that will require an additional measure to control buckling e.g. encasing the dissipating haunch element in a buckling restrained tube filled with concrete, which is in principle similar to buckling restrained braces. Figure 5 show details of stiffer and dissipating haunch designed based on the analysis of connection of the considered frame, and following the aforementioned design procedure. The preliminary designed connections were modeled in the FE based nonlinear analysis software SeismoStruct for verification, which ensured beam flexure yielding under lateral loads.

3 Shake table testing of as-built and retrofitted test models

3.1 Preparation of 1:3 reduced scale models

For simplicity reason and due to the fact that scaling stress–strain properties of both concrete and steel re-bar materials for model preparation are quite demanding and costly, a simple model idealization was considered in which the materials' stress–strain properties essentially remained the same for both the prototype and models (Ahmad et al. 2019). Following the simple model idealization all the linear dimensions of beams, columns and slabs and diameter of the steel re-bars were reduced by a scale factor S_L 3. Concrete for the 1:3 reduced scale model was prepared with a mix proportion of cement, sand and 3/8 in. (9 mm) down coarse aggregate to respect the aggregate scaling requirements for concrete. The ACI concrete mix design procedure was followed for the preparation of concrete with compressive strength of 3000 psi (21 MPa) for Model-1 and 2000 psi (14 MPa) for Model-2 to Model-5. A mix proportion of 1:1.80:1.60 (cement: sand: aggregate) with a water-to-cement ratio of 0.48 is used to achieve 3000 psi (21 MPa) and mix proportion of 1:3.50:2.87 (cement: sand: aggregate) with a water-to-cement ratio of 0.80 is used to achieve 2000 psi (14 MPa).

The construction of models was carried in series under the strict supervision of site engineer. Initially special steel formworks were designed and prepared for all the components including structure's base pad (footing), columns and slab with provisions

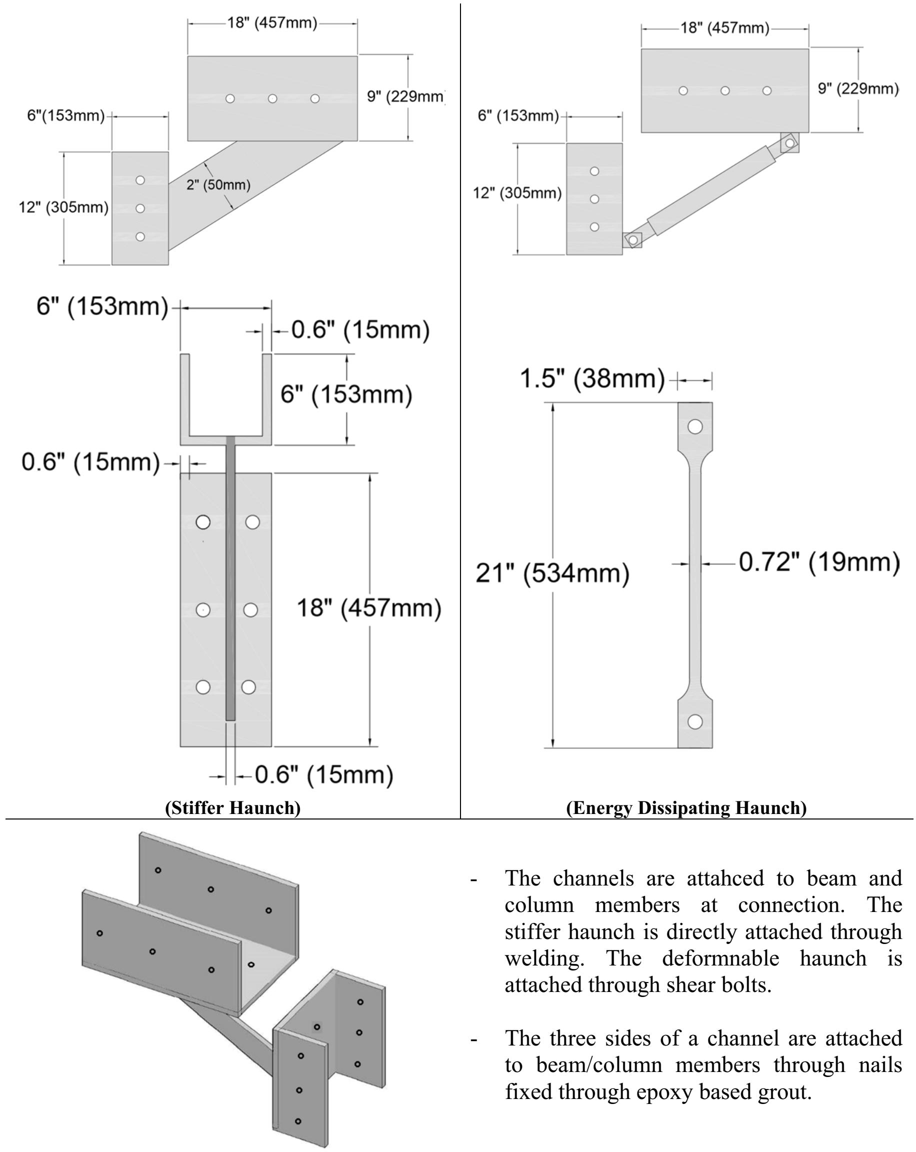

Fig. 5 Details of stiffer and dissipating haunch designed for the considered frame

for in-plane and transverse beams. The construction sequence included the preparation of reinforced concrete base pads 22 in. width × 15 in. depth × 8 feet length (559 mm × 381 mm × 2439 mm) for all the models one after the other, which were cured for 14 days with moist bags. It was followed by the construction of columns, construction of in-plane and transverse beams and slab monolithically for each of the model in series, which were cured for 14 days. In similar fashion the next story columns, beams and slab were constructed and cured. This way all the five models were prepared in time duration of about 4-1/2 months.

It is worth to mention that the model and prototype uses essentially the same materials type (concrete and steel re-bars), which have similar stress–strain behavior and material density (unit weight). Due to the above, the reduced scale models were subjected to gravity and seismic mass less than the required as per the similitude requirements for prototype-to-model conversion:

$$M_r = \frac{M_M}{M_P} = L_r^2; \quad L_r^2 = \frac{1}{S_L^2} \tag{1}$$

where M_r is the ratio of model mass M_M to prototype mass M_P, L_r is the reciprocal of linear scale factor S_L. In order to satisfy the above requirements for complete model mass simulation, the additional required mass were applied to each floor of the model, calculated following the mass simulation model of Quintana-Gallo et al. (2010):

$$M_{M1} = \frac{M_P}{S_L^2} - M_{M0} \tag{2}$$

where M_{M1} is the additional floor mass for model, M_{M0} is the floor mass of model. The total mass on each floor is, thus, the sum of additional mass M_{M1} and M_{M0}. The additional floor mass (1200 kg for each floor) was simulated through two 600 kg steel blocks, prepared by stacking and welding steel plates together, which were mounted and fixed to the floor by means of fully secured ½ in. (13 mm) steel bolts.

In the present research both the rigid and deformable, energy dissipating, haunch types were considered for retrofitting of the considered deficient frames. Focus was particularly made on modifying the design scheme of stiffer haunch proposed by Sharma et al. (2014), and scheme of application on structure (i.e. haunch applied below beam, and haunch applied both below and above beam), additionally a nonlinear deformable haunch with restrained buckling was further included in the research to explore possibility of e nergy dissipation through deformable haunch that add supplemental damping to the structure, beside avoiding joint panel damage under seismic excitation. The stiffer haunch were fabricated from the steel plates whereas the dissipating haunch were fabricated and encased in stiffer circular steel tubes that were filled with concrete to avoid buckling of the deformable haunch element under compression loading. Figure 6 shows the application schemes considered herein. On average, the overall cost of haunch

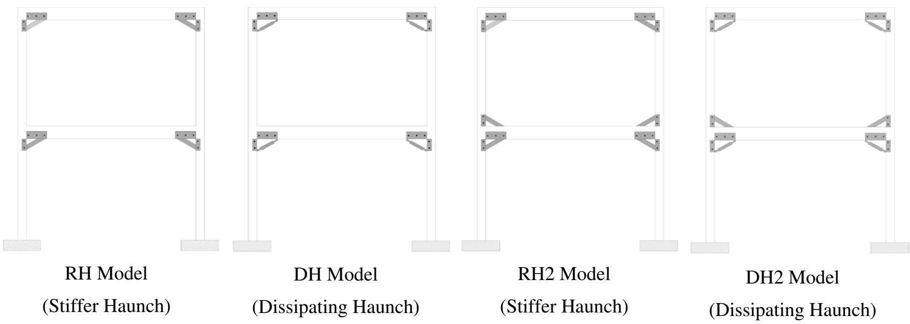

Fig. 6 Application schemes of haunch retrofitting of RC frames (Model 3 and Model 5, ref. Table 1)

retrofitting per location (per haunch) is about Rs. 950.0 (≈ 10.0 USD) for the model, which can reach to about Rs. 2500 (≈ 25.0 USD) for the prototype. The indicated composite cost included cost for all material types (steel plates, welds, epoxy, nails) and accessories, and also included labor cost.

3.2 Test setup and instrumentation

The model was lifted through a 20-ton overhead crane, placed on the shake tabletop and secured firmly by means of 18 steel bolts ½ in. (13 mm) diameter. The over-hanged portion of the base pad was placed on a specially fabricated roller support, comprised of 4-leg steel stool that was provided with 4#8 (4φ25 mm) steel rods to allow model lateral movement during testing. The test model was instrumented with six accelerometers with maximum capacity of ± 10 g and three displacement transducers with maximum capacity of 24 in. (610 mm). Two uni-axial accelerometers (front and back) were installed on each floor and base pad to record the in-plane acceleration of the model. For in-plane lateral displacement measurements, a fixed steel reference frame was erected in-lined with the model. The displacement transducers were mounted on the reference frame; the transducers' strings were stretched by half-length of 12 in. (305 mm) and attached to each floor and base pad, keeping the table positioned at mid-way of ± 125 mm displacement.

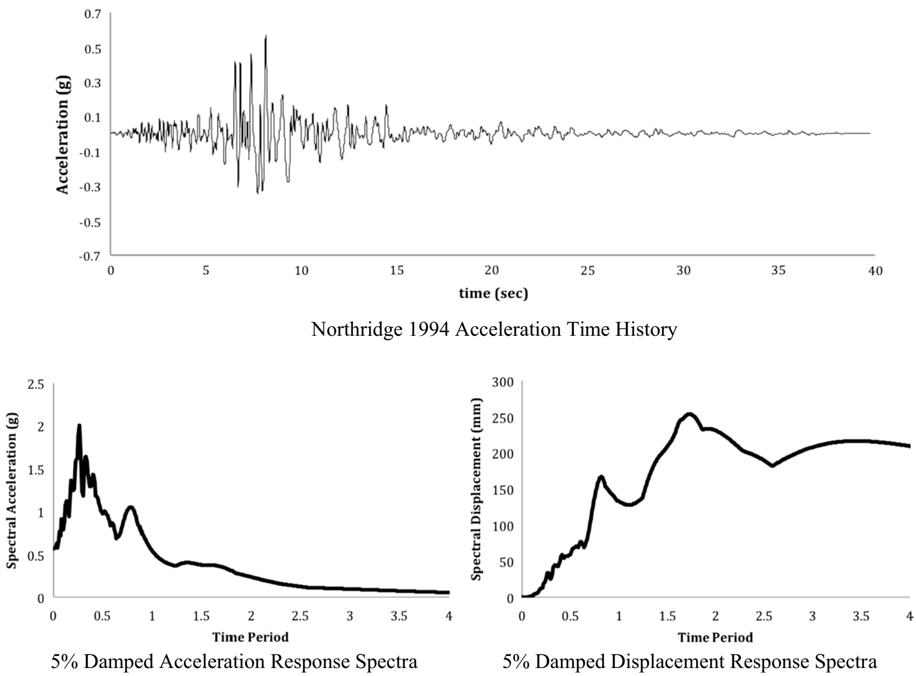

Fig. 7 Selected acceleration record for shake table testing

3.3 Input excitation and loading protocols

A natural acceleration time history (accelerogram) of 1994 Northridge earthquake (horizontal component, 090 CDMG Station 24278 - PEER strong motion database, blind thrust faulr) was selected as an input excitation after careful analysis of number of accelerograms (Fig. 7). This record has maximum acceleration of 0.57 g, maximum velocity of 518 mm/s and maximum displacement of 90 mm, generated over a blind thrust fault with shallow depth of about 18 km. After the shake-table self-check run for system adjustment, the selected acceleration time history was applied to the test model with multiple excitations—5%, 10%, 20%, 30%, 40%, 50%, 60%, 70%, 80%, 90%, 100% and 130% of the maximum acceleration of record, to push the structure from elastic to inelastic and severe damage state. Each of the model was tested progressively and its damage behavior was observed after every run, the tests were concluded when the test models were found in the incipient collapse state.

3.4 Observed behaviour of tested models

3.4.1 Observed behavior and damage evolution, as-built models

The code compliant model (Model-1) was observed with beam-sway mechanism; experiencing flexure yielding at the beam ends and slight flexure cracking at bottom end of columns on the ground story under test run with 100% intensity of excitation i.e. design level earthquake excitation. This model was able to resist 130% of Northridge record for collapse limit state exceedance, deforming to 5.30% roof drift with max. force resistance of 255 kN. Model-2 to Model-5 were observed with flexure cracking in both columns and beams and severe damages in joint panel regions under input excitation well below the design level excitation. Considering the ultimate limit state (incipient collapse state), Model-2 deformed to 5.0% drift with max. force resistance of 180 kN, Model-3 deformed to 4.77% drift with max. force resistance of 185 kN, Model-4 deformed to 3.45% drift with max. force resistance of 152 kN, Model-5 deformed to 3.92% drift with max. force resistance of 125 kN. Figures 8, 9 and 10 shows the typical damages observed in the deficient models. The use of low strength concrete lowered the structure resistance and altered the mechanism from beam-sway to column-sway and joint mechanism. In addition, the lack of confining ties in joint panel region resulted in the joint panels' concrete cover spalling under lateral excitations well below the 100% intensity of Northridge record. Damage evolution was deduced for each tested model, describing the observed local damages in structural components correlated with lateral roof drift and base shear force. Tables 2 and 3 shows the damage evolution of Model-3 and Model-5, which were further considered for retrofitting.

3.4.2 Observed behavior and damage evolution, haunch retrofitted models

The application of haunch at the beam-column connection altered the initial mechanism, forming flexure hinging in beams and columns at distance from the beam-column interface; the flexure cracking in beams and columns distributed over significant length (Fig. 11). However, damages were experienced also in the joint panel regions upon subjecting the

Flexure Cracks in Beams and Columns, Ground Storey

Slight Cracks in Joint Panel on Ground Storey

Damages Observed in Columns, Beam and Joint Panels during 5% Run

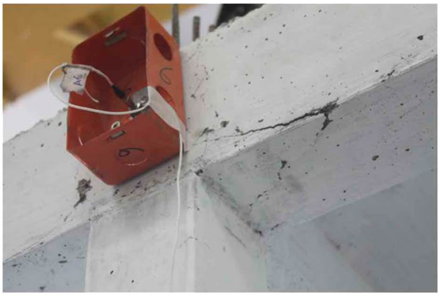

Severe Bat-Like Cracks in Joints on First Storey

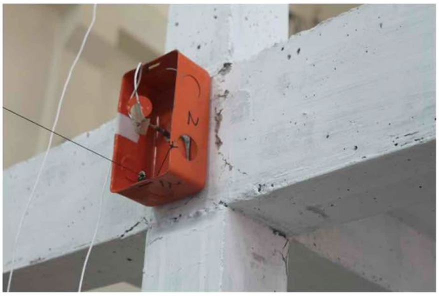

Damage Progress in Joint Panel on Ground Storey

Damages Observed in Joint Panels of Ground and First Storey during 30% Run

Cover Detachment and Damage in Joint on First Storey

Severe Damage to Joint Panel on Ground Storey

Damages Observed in Joint Panels of Ground and First Storey during 40% Run

Fig. 8 Observed damages in Model-3, refer Table 1 for damage evolution

structure to larger lateral displacement under extreme shaking (Fig. 12). This resulted due to the pullout of haunch from column during extreme shaking causing connection opening, which happened due to the inevitable detachment of a wedge like concrete from column due to the low strength of concrete providing lower resistance against prey out. Figure 11


Flexure Cracks in Beam and Column on Ground Storey   Cracks in Top Ends of Columns on First Storey

Damages Observed in Beams and Columns during 5% Run


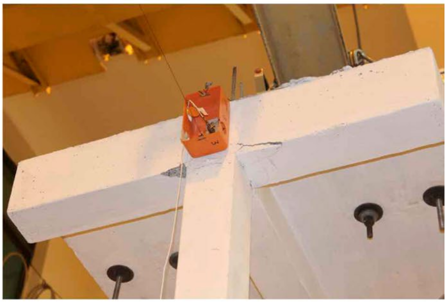

Concrete Crushing at Column Top Ends, Ground Storey   Cover Concrete Detachment from Joints on First Storey

Damages Observed in Column Ends on Ground Storey and Joint Panels of First Storey during 50% Run


Extend of Damage to Joints on Ground Storey   Extend of Damage to Joints on First Storey

Damages Observed in Joint Panels of Ground and First Storey during 60% Run

Fig. 9 Observed damages in Model-5, refer Table 2 for damage evolution

and 12 shows the extent of damage observed in beam-column joint regions upon subjecting the model to extreme level shaking, and Tables 4, 5 and 6 reports the damage evolution of the retrofitted model. This damage is relatively more severe in model where haunch is applied only below the beam at the connection. Because, the strain in the longitudinal

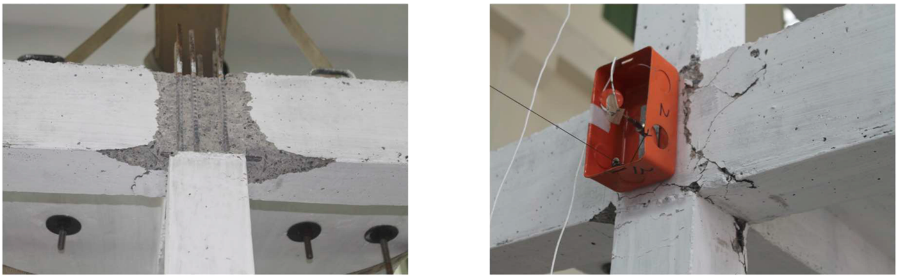

Top Story Joint First Story Joint

(a) *Model-3, special moment frame built in low strength concrete and lacking confining ties in joints*

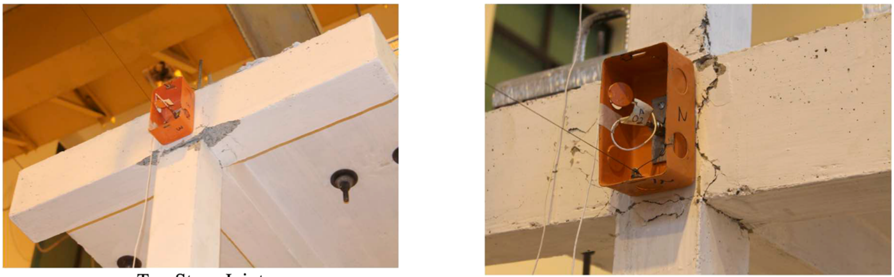

Top Story Joint First Story Joint

(b) *Model-5, moment frame built in low strength concrete, lacking confining ties in joints and having reduced longitudinal and transverse reinforcements*

Fig. 10 Observed damages in joint panel regions at the incipient collapse state

re-bars of columns at the bottom ends penetrate through the joints under tension loading, resulting in stress demand on panel zone. The shaking induced stress demand in joint panel can result into joint damage upon exceeding the joint principal tensile strength (Priestley 1997; Pampanin et al. 2002).

4 Fragility functions and vulnerability curves

4.1 FE based structural modelling of RC frame

For inelastic modeling and seismic analysis of the considered structures, the FE based software SeismoStruct (SeismoSoft 2016; Pinho 2007), as proposed earlier (Ahmad et al. 2018), has been adopted and further extended herein for generalization, and also it is validated against further experimental shake table tests on RC frames. SeismoStruct is employed to model the considered reinforced concrete frames, idealized as an equivalent frame (Fig. 13), and provisioned with lumped plasticity hinges; at the beam-ends for re-bar slip (Rashid and Ahmad 2017), at the beam-column panels for joint shear hinge simulation. Haunches were modeled using the inelastic truss type element, connected to beams and columns through rigid links.

The joint shear strength τ_j can be calculated using available analytical model developed based on the experimental and numerical research (Kurose 1987; Priestley 1997; Pampanin et al. 2002; Kim and LaFave 2012) for both non-seismic (gravity) and seismically designed

Table 2 Observed response and damage evolution of Model-3, as-built model

Run	Roof displacement inch (mm)	Roof drift (%)	Base shear kips (kN)	Observed damages
5%	4.87 (123.69)	(1.75)	26.51 (117.92)	Slight cracks were observed at the base of columns on the ground sotrey and significant flexure cracks at the base of columns on the first storey A bat-like diagonal cracks were observed in the joint panels on ground storey and slight diagonal bat-like cracks in the joint panels on first storey Flexure cracks and slight vertical cracks were observed also at the beam-ends on both the ground storey and first storey
30%	7.18 (182.365)	(2.57)	30.91 (137.48)	Existing damages in the model were aggravated Flexure cracks at the base of columns were widened on both the ground storey and first storey Flexure and vertical cracks at beam-ends significantly widened in beam on ground storey Damages in the joint panels on ground storey were further aggravated Extreme damages were observed in joints on first storey, with a clear bat-like concrete wedge about to detach from the joint panels
40%	13.31 (338.19)	(4.77)	41.48 (184.50)	Concrete crushing at the top and bottom ends of columns on both the ground storey and first storey, with minor spalling at the base of columns Damages in the joint panels on the ground storey further increased and observed with minor cover concrete spalling from the joint panel Joint panels on the first storey were severely damaged and observed with cover concrete wedge detachment and spalling The model after this run was found in the incipient collapse state

Table 3 Observed response and damage evolution of Model-5, as-built model

Run	Roof displacement inch (mm)	Roof drift (%)	Base shear kips (kN)	Observed damages
5%	1.01 (25.65)	(0.36)	8.08 (35.96)	Slight flexure cracks appeared at the top and bottom of columns on both the ground storey and first storey Slight flexure cracks were also observed at the beam-ends on ground storey
30%	3.66 (92.95)	(1.31)	18.73 (83.31)	During this run the existing cracks in the model were further widened
50%	10.93 (277.60)	(3.92)	28.07 (124.84)	Cover concrete were crushed and observed with minor spalling at the top of columns on both the ground storey and first storey Flexure cracks at the beam-ends on ground storey were further aggravated and significant vertical cracks also appeared at the beam-column interface on ground storey Significant diagonal cracks were appeared in the joint region on both the ground storey and bottom storey. However, damage to joints on top storey was comparatively more severe A bat-like cover concrete was detached from the top joints

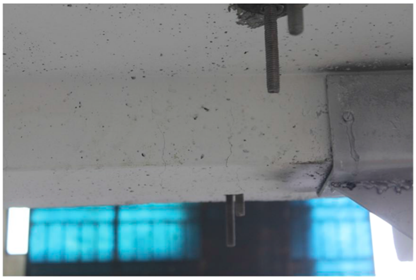

Plasticity distribution in beam

Plasticity distribution in column

(a) *Haunch Retrofitted Model-5, moment frame built in low strength concrete, lacking confining ties in joints and having reduced longitudinal and transverse reinforcements*

Detachment of haunch under extreme shaking

Joint cracks/connection opening under extreme shaking

(b) *Haunch Retrofitted Model-5, moment frame built in low strength concrete, lacking confining ties in joints and having reduced longitudinal and transverse reinforcements*

Fig. 11 Observed damages in deficient models retrofitted with haunch

frames. The present research adopted the analytical model proposed by Kim and LaFave (2012), which has been developed and validated against numerous experimental researches, to model the spring limit state strength and deformability capacity for the adopted multi-linear constitutive law of Sivaselvan and Reinhorn (2001), as shown in Fig. 14. Kim and LaFave (2012) have proposed a shear strength-shear deformability model that largely depends on the geometry of the joint, compressive strength of concrete, longitudinal reinforcement of beam and transverse reinforcements in joint panel region. For peak shear strength:

$$\tau_j(\mathrm{MPa}) = \alpha_t\beta_t\lambda_t(JI)^{0.15}(BI)^{0.30}(f'_c)^{0.75} \tag{3}$$

where α_t is the in-plane geometry parameter, which is 1.0 for interior, 0.7 for exterior and 0.4 for knee connection; η_t is the joint eccentricity parameter equal to $(1-\mathrm{e}/\mathrm{b}_c)^{0.67}$; β_t is the out-of-plane geometry parameter, which is 1.0 for subassemblies with zero or one transverse beam and 1.2 for subassemblies with two transverse beams; λ_t is an adjusting factor to set the overall average of the ratio, it is equal to 1.31; $f_c^{'}$ is the concrete compressive strength; $JI=(\rho_j\times f_{yj})/f_c^{'}$ is the joint transverse reinforcement index, where ρj is the volumetric joint transverse reinforcement ratio in the direction of loading and f_{yj} is the yield stress of joint transverse reinforcement; $BI=(\rho_b\times f_{yb})/f_c^{'}$ is the beam reinforcement index, where ρ_b is the beam reinforcement ratio and f_{yb} is the yield stress of beam reinforcement.

The shear deformation corresponding to peak shear strength model proposed by Kim and LaFave (2012) is formulated:

$$\gamma_j(rad.) = \alpha_{\gamma t}\beta_{\gamma t}\eta_{\gamma t}\lambda_{\gamma t}BI(JI)^{0.30}\left(\frac{\tau_j}{f'_c}\right) \tag{4}$$

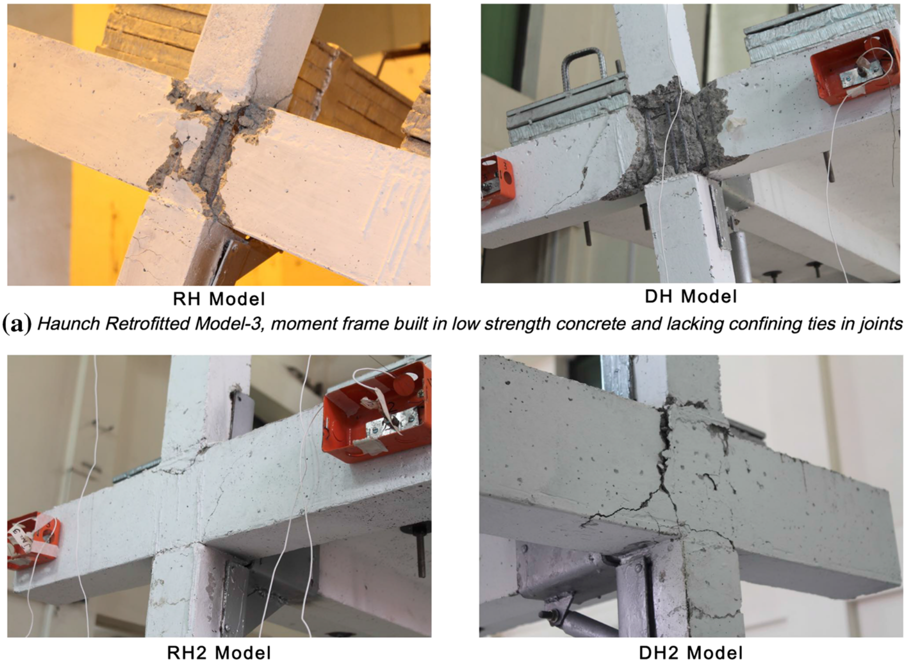

(a) *Haunch Retrofitted Model-3, moment frame built in low strength concrete and lacking confining ties in joints*

(b) *Haunch Retrofitted Model-5, moment frame built in low strength concrete, lacking confining ties in joints and having reduced longitudinal and transverse reinforcements*

Fig. 12 Observed damages in haunch retrofitted RC frames with different application schemes, after haunch pullout due to concrete pry-out

where $\alpha_{\gamma t} = (JPRU)^{2.1}$ is the parameter for describing in-plane geometry, where *JP* represents the ratio of number of not-free in-plane surfaces around a joint panel to the total number of in-plane surfaces of the joint panel, to consider possible changes in joint shear strength according to in-plane geometry; *JP* is 1.0 for interior connections, 0.75 for exterior connections, and 0.5 for knee connections; $\eta_{\gamma t}$ is the joint eccentricity parameter equal to $(1 - e/b_c)^{-0.6}$, which is 1.0 for no eccentricity; $\beta_{\gamma t}$ is the out-of-plane geometry parameter, which is 1.0 for subassemblies with zero or one transverse beam and 1.4 for subassemblies with two transverse beams; $\lambda_{\gamma t} = 0.0055$ is an adjusting factor to set the overall average of the ratio.

The above shear-deformation models, Eqs. (3) and (4), gives estimate of maximum shear and corresponding deformation in joint panel, shear-deformation for the other limit states can be obtained using the proposed empirically derived factors given in Table 7. The limit state's shear stress computed was put in the Eq. (9) to calculate the corresponding limit state's moment capacity for shear simulation hinge (Fig. 14).

4.2 Test and validation of the numerical modelling technique

The representative prototype of the tested RC frame is prepared in FE based software SeismoStruct (Fig. 15), following the aforementioned modeling approach to idealize the structural components (in-plane and transverse beams, columns and beam-column joint panels). Structural beam-column members' geometric and material properties are defined

Table 4 Observed response and damage evolution of Model-3, haunch retrofitted, stiffer haunch applied only below the beam at the connection

Run	Roof displacement inch (mm)	Roof drift (%)	Base shear kips (kN)	Observed damages
70%	7.10 (180.30)	(2.6)	39.01 (173.53)	Flexure cracks were observed at the top and bottom of columns on ground storey Flexure hinging at the base of column on first storey Slight shear cracks in joint region on ground storey
80%	8.60 (220.68)	(4.9)	43.80 (194.82)	Severe flexure cracks were observed at the bottom of column on ground storey along with concrete spalling Severe shear cracks in joint region with concrete spalling on ground storey Slight shear cracks in joint panel on first storey The model after this run was found in the incipient collapse state

Table 5 Observed response and damage evolution of Model-5, haunch retrofitted, stiffer haunch applied both below and above the beam at the connection

Run	Roof displacement inch (mm)	Roof drift (%)	Base shear kips (kN)	Observed damages
50%	4.63 (117.52)	(1.53)	26.86 (119.46)	Slight flexure cracks were observed throughout the length of ground storey column A shear crack was observed in the joint panel on ground storey
60%	6.52 (165.54)	(2.36)	32.49 (144.52)	Existing cracks in the model were slightly widened Flexure cracks both at the top and bottom of the first storey columns were observed Pullout of haunch initiated from column at the bottom of first storey columns
70%	11.34 (287.94)	(4.50)	41.43 (184.27)	Existing damages in the model were aggravated Flexure cracks were observed in beam at the haunch application location Shear cracks in joint panel at ground storey were observed Chunk of concrete along with haunch pulled out from column at the bottom ends on first storey
80%	13.70 (348.88)	(6.40)	44.47 (197.80)	Buckling of re-bars at the base of columns on ground storey was observed Chunk of concrete along with haunch initiated separation at the top ends of columns on both ground storey and first storey Shear cracks in joint panel aggravated. Spalling of cover concrete was observed at the joint panel on ground storey The model after this run was found in the incipient collapse state

Table 6 Observed response and damage evolution of Model-5, haunch retrofitted, energy dissipating haunch applied both below and above the beam at the connection

Run	Roof displacement inch (mm)	Roof drift (%)	Base shear kips (kN)	Observed damages
Self-check	2.64 (67.07)	(1.13)	22.49 (134.62)	Slight flexure cracks were observed at the column base on ground storey Slight flexure cracks were observed also at the columns top ends on both ground and first storey
80%	7.18 (182.365)	(2.57)	30.91 (137.48)	The existing flexure cracks in columns were widened and further flexure cracks appeared in the column on ground storey Slight shear cracks appeared in joint region on ground storey Diagonal cracks were observed in transverse beams on ground storey, starting from top haunch interface to bottom side
90%	13.31 (338.19)	(4.77)	41.48 (184.50)	The existing cracks were further aggravated Significant flexure cracks were observed at the base of column on ground storey Existing shear cracks in joint panel region on ground storey widened significantly with appearance of additional cracks Cracks in transverse beams further widened, and additional cracks appeared Significant spalling of cover concrete is observed in the joint panel region on ground storey Concrete cover spalling was also observed at the base of columns on ground storey Haunch was completely pulled out from column at the bottom ends on first storey

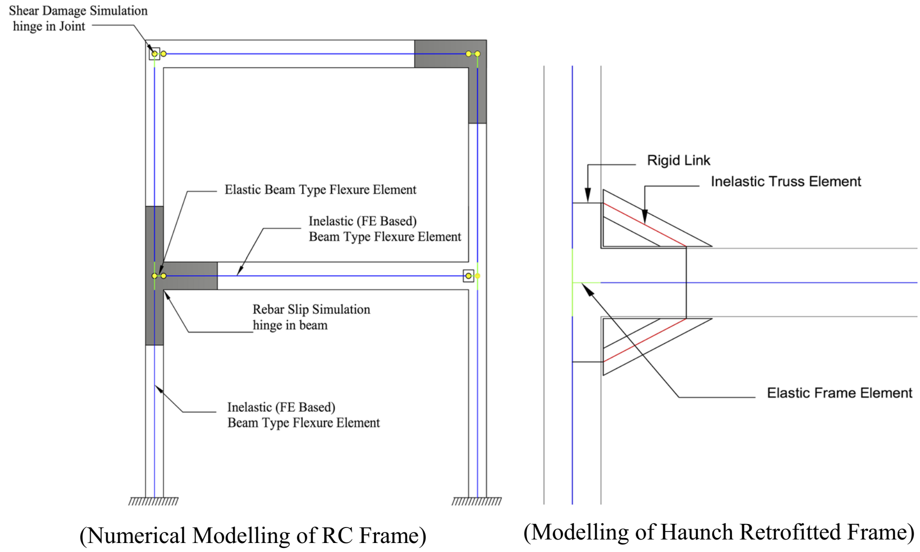

Fig. 13 Inelastic modeling of reinforced concrete frame for numerical analysis

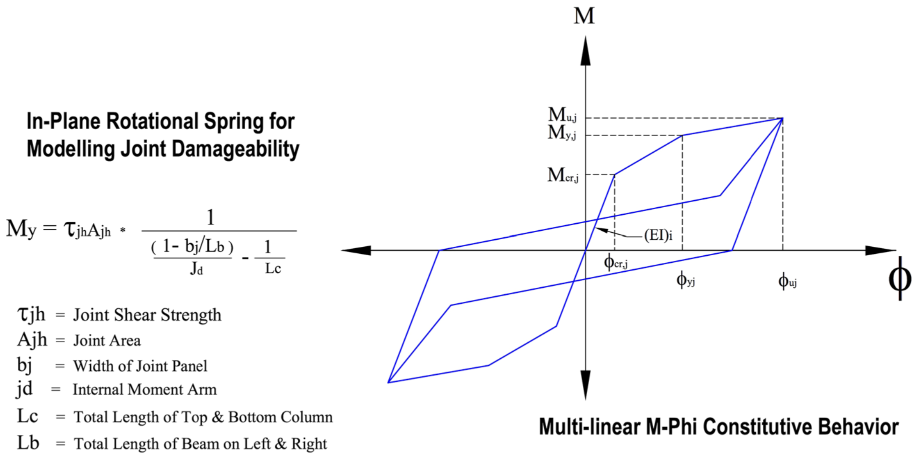

Fig. 14 Constitutive relationship for joint shear hinge. Limit states' moments are computed for the corresponding shear using Eq. (3) and using the Sivaselvan and Reinhorn (2001) constitutive model given in SeismoStruct

for each model. Similarly, the joint limit state shear stress and deformation are calculated for each model and transformed to corresponding moment-rotation (Celik and Ellingwood 2008; Alath and Kunnath 1995; Biddah and Ghobarah 1999; Youssef and Ghobarah 2001; Lowes and Altoontash 2003). In case of code conforming model, materials' overstrength is considered as proposed by Priestley et al. (2007). The frame was subjected to the considered imposed loading on floors and subjected to input excitation (acceleration) that was recorded at the base of the model. The response of each model was recorded in terms of

Table 7 Limit state shear and deformation for joint panel, as proposed by Kim and LaFave (2012), used for constitutive law of shear-hinge simulation spring (Fig. 14)

Parameters	Cracking		Yielding		Maximum	
	τ_{cr}	Std.	τ_{y}	Std.	τ_{max}	Std.
τ (MPa)	$0.442\times\tau_{j(max)}$	0.299	$0.890\times\tau_{j(max)}$	0.154	$\tau_{j(max)}$	0.153
γ (rad.)	$0.0197\times\gamma_{j(max)}$	0.437	$0.362\times\gamma_{j(max)}$	0.420	$\gamma_{j(max)}$	0.410

The peak values are obtained using Eqs. (3) and (4)

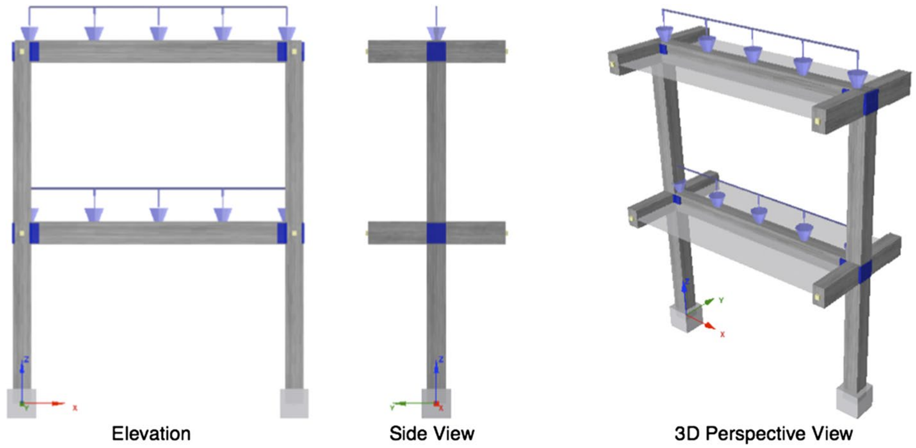

Fig. 15 FE based representative prototype structure prepared in SeismoStruct

roof displacement time history, peak lateral displacement and peak base shear force, and local damage mechanism (beam bar-slip and joint damage). Figure 16 shows the comparison of numerical analysis using SeismoStruct to the experimentally observed roof displacement time history response for as-built frames, Table 8 reports the comparison of numerically obtained peak displacement and peak base shear force to experimentally observed.

It can be observed that the numerical models predict the roof displacement time history response in a reasonable agreement to the experimentally observed response: in terms of the displacement response following the same trend, the occurrence of displacement peaks, and the alternate rise and decay in displacement response. The comparison reveal an error of about 10% in numerically predicting the lateral displacement and an error of about 5% in predicting the base shear force. In comparison to the deficient RC frames, the percentage of error is less in case of code conforming model. This reasonable prediction of global performance of RC frame structures shows soundness of the proposed modeling technique and the FE based tool SeismoStruct in simulating the dynamic seismic response of reinforced concrete frame structures experiencing beam bar-slip and joint panels damageability.

For haunch retrofitted frames, Model-3 and Model-5 are considered and provisioned with haunches in similarly fashion as discussed earlier, however considering all sources of inelasticity i.e. inelasticity in beam-column members, beam bar-slip, joint panel damageability and inelastic haunches, which were modeled as inelastic truss element. Figure 17 shows the comparison of numerically predicted to experimentally observed

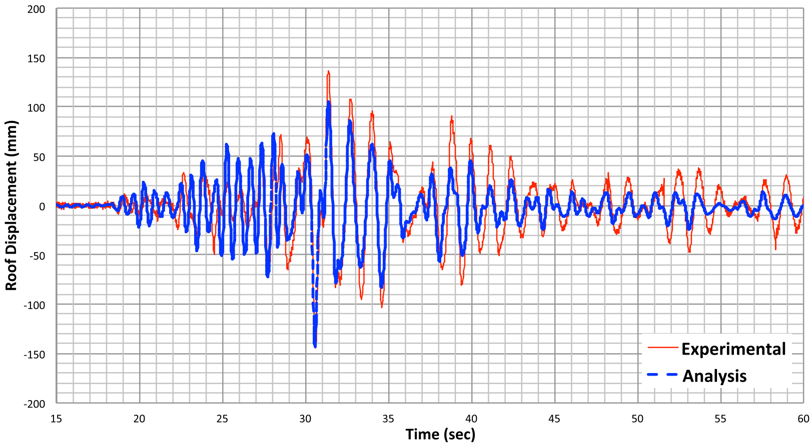

Model-1 (Code Conforming), 2% roof drift (exp.)

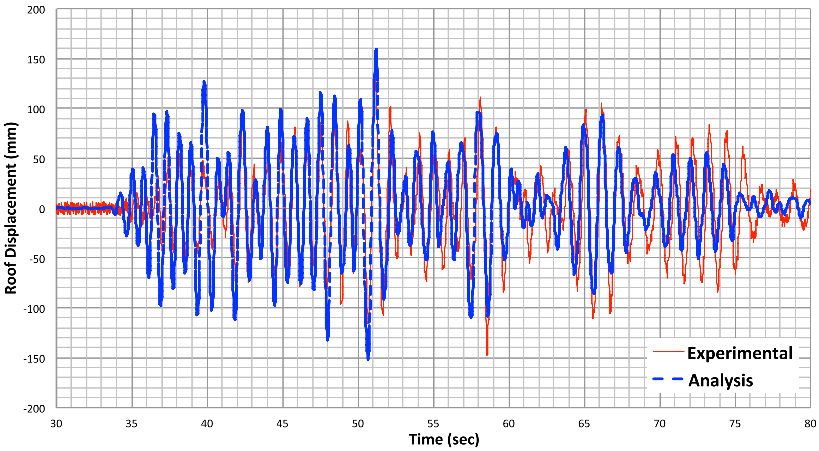

Model-2 (RC in low strength concrete), 2% roof drift (exp.)

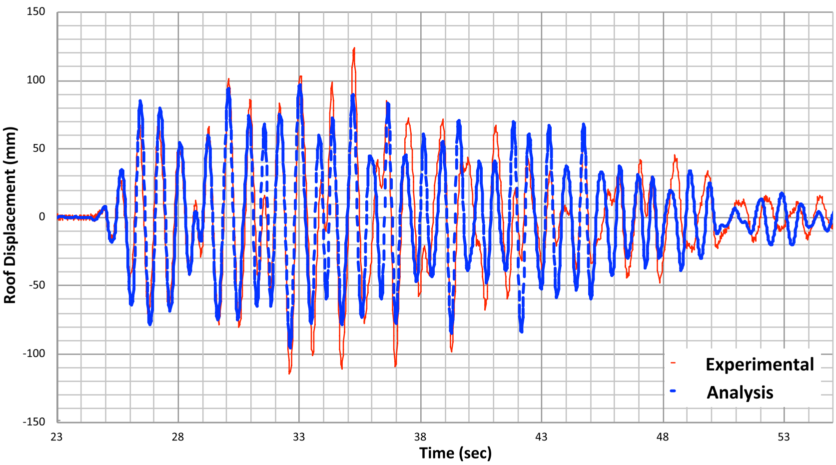

Model-3 (RC in low strength concrete, lacking ties in joints), 1.75% roof drift (exp.)

Fig. 16 Roof displacement time history response of RC frames, as-built models

Table 8 Numerical to experimental prediction using FE-based software SeismoStruct

Model	Lateral roof displacement (mm)		Base shear force (kN)		Error (%), Num-to-Exp	
	Numerical	Experimental	Numerical	Experimental	Displacement	Base shear
As-built RC frame models						
Model-1	144.31	145.12	166.26	205.25	0.56	19.00
Model-2	159.99	147.93	148.74	163.57	−8.15	9.07
Model-3	96.77	123.69	110.86	117.92	21.76	5.99
Model-4	143.87	150.23	132.55	135.82	4.23	2.41
Model-5	93.82	110.00	95.21	70.81	14.71	−34.46
				Avg.	6.62	0.40
Haunch retrofitted RC frame models						
RH	107.66	129.46	153.36	147.51	16.84	−3.97
RH2	135.21	117.38	113.27	119.47	−15.19	5.19
DH2	95.95	106.44	99.98	117.95	9.86	15.24
				Avg.	3.83	5.49
				Combined Avg.	5.23	2.94

roof displacement response for models retrofitted with haunch. It can be observed that numerical analysis is reasonably in agreement with the experimental observation, however, in case of the Model-5 retrofitted with stiffer haunch, numerical analysis experience a permanent offset after the peak response is observed. It is due to the fact that the ground-story column experience irrecoverable plastic deformation for this model. Numerically predicted peak response is in a good agreement but with a little over prediction, also, the residual deformation observed in numerical analysis is relatively higher than the experimental, nevertheless, it is conservative for vulnerability assessment. Table 8 also reports the error in numerical to experimental prediction for roof displacement and base shear force, on average, which is about 5.23% for displacement and 2.94 for base shear force for all the models.

4.3 Incremental dynamic seismic analysis and derivation of fragility functions

Incremental dynamic seismic analysis (IDA) technique, as proposed earlier by Vamvatsikos and Cornell (2002) for structure's dynamic response analysis and derivation of seismic response curve, and the probabilistic-based nonlinear dynamic reliability based method (NDRM) of Ahmad et al. (2014) are considered for the derivation of fragility functions of the considered as-built and retrofitted RC frame structures. A suit of seven ground motion records were obtained from the PEER NGA strong ground motions database, having moment magnitude M_W in the range of 6–7.5 and source-to-site distance of 10–30 km. Table 9 reports the selected ground motion records, which are carefully selected taking into account the event-to-event and region-to-region variability, and being compatible with the regional tectonics. The selected ground motion records were scaled and matched to the design acceleration spectrum through wavelet-based approach incorporated in SeismoMatch (2016). The matched accelerograms were retrieved and linearly scaled up/down to multiple intensity levels for structures' incremental seismic analysis in order to retrieve

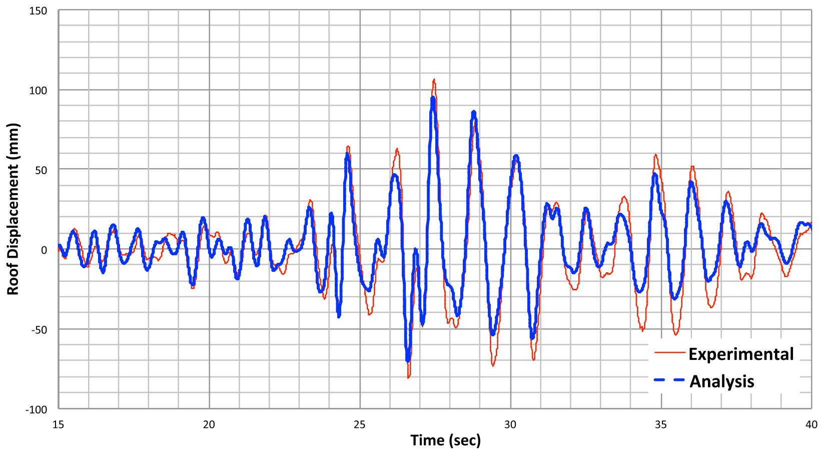

Model-5 Retrofitted with Dissipating Haunch (DH2), 1.50% roof drift (exp.)

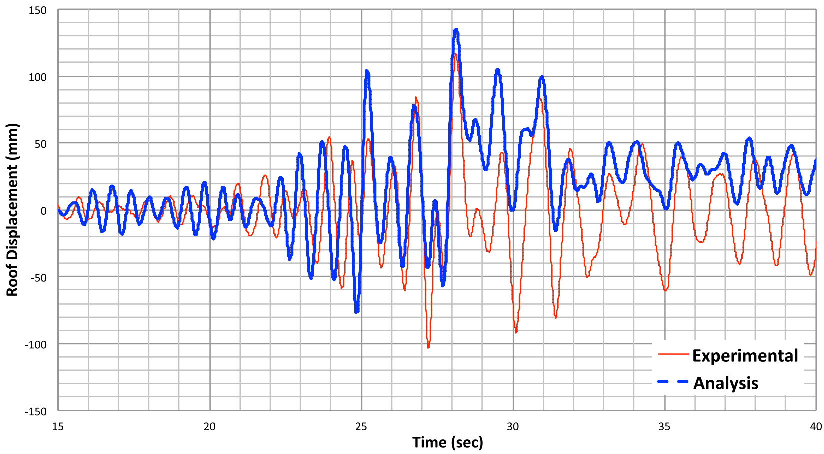

Model-5 Retrofitted with Rigid Haunch (RH2), 1.66% roof drift (exp.)

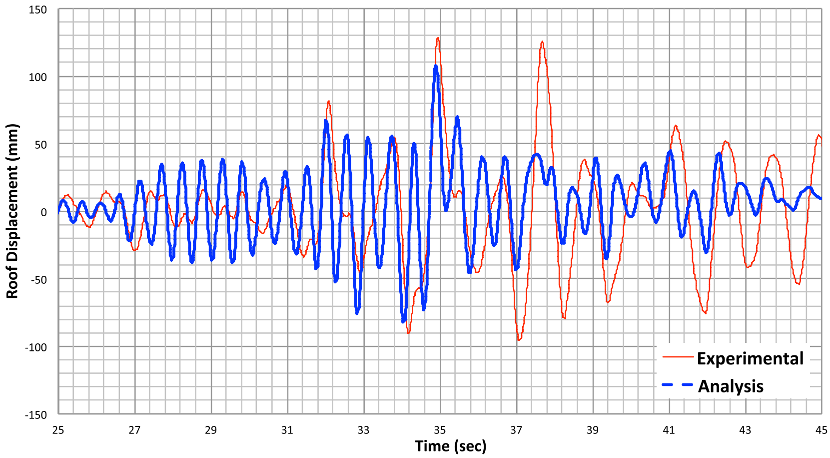

Model-3 Retrofitted with Rigid Haunch (RH), 1.83% roof drift (exp.)

Fig. 17 Roof displacement time history response of RC frames, retrofitted models

Table 9 Ground motion records extracted from the PEER NGA strong ground motions database, used for incremental dynamic seismic analysis of structures

GM record	Year	Event	Station	M_W	PGA (g)
1	1978	Tabas, Iran	Boshrooyeh	7.35	0.252
2	1989	Loma Prieta, USA	Hollister	6.93	0.240
3	1995	Kobe, Japan	Abeno	6.90	0.327
4	1988	Spitak, Armenia	Gukasian	6.77	0.300
5	1980	Victoria, Mexico	Chihuahua	6.33	0.235
6	1983	L'Aquilla, Italy	Avezzano	6.30	0.256
7	1984	Morgan Hill, USA	Agnews State Hospital	6.19	0.220

the seismic response demand parameters (roof displacement), which is correlated with the seismic intensity to derive the structures' response curves, which are employed for the calculation of limit state probability exceedance for specified seismic intensities.

Both for as-built and haunch retrofitted structures, two-storey representative prototype structure models were considered and numerically modeled in SeismoStruct, like-wise Fig. 15, considering detailing that of Model-3 and Model-5 and their counterpart haunch retrofitted models. Haunch applied at the connection both below and above the beam are considered for Model-5 whereas haunch applied only below the beam is considered for Model-3. Furthermore, since the hysteretic-based energy-dissipating haunch, as designed earlier, has very much similar seismic response in comparison to the stiffer haunch, thereby, only the latter is considered for onward seismic analysis and derivation of fragility functions. Both the as-built and retrofitted structures were analyzed through IDA using the selected accelerograms. Roof displacement response demand under each ground motion record was correlated with the

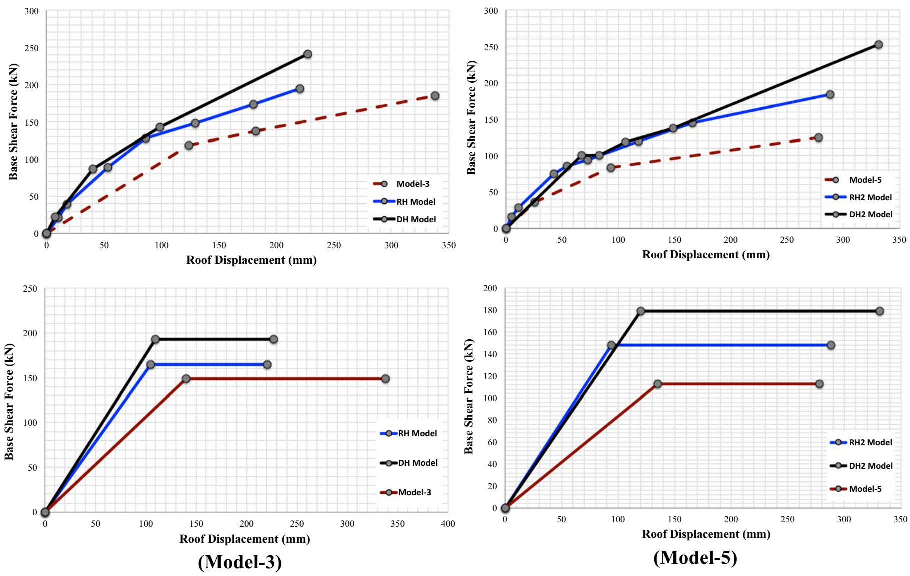

Fig. 18 Lateral force-deformation response of as-built and retrofitted RC frame obtained experimentally and the idealized bi-linear force-displacement capacity curves

base shear force and seismic intensity in order to derive capacity curves and seismic response curves respectively (Ahmad et al. 2014, 2018).

For derivation of fragility functions, the NDRM method requires structure-specific damage scale to calculate the limit states' probability of exceedance. A unified procedure was adopted to develop damage scale for each structure, which specifies the limit states' drift capacity given the structures' idealized yield and ultimate drift capacities. Figure 18 shows the experimentally obtained force-displacement curves and the idealized bi-linear curves derived based on the energy balance criterion in order to calculate the structures' idealized yield displacement.

Upon exceedance of the yield displacement, most of the structures initiate cracking/damage in the structural components (i.e. beams, columns, joint panels). The ultimate drift capacity of structures is based on the experimentally observed maximum drift capacity at the incipient collapse limit state, essential for the collapse assessment of the structures. Additionally, code specified 2.50% allowable drift limit is also considered for all the structures that correspond to the occurrence of significant damage in the structural components, and essential for the structural performance assessment. For a target seismic intensity level, the roof displacement demand vector is obtained for the time history analysis for all the records, which is convolved with the limit-states' roof displacement capacity obtained experimentally (Table 10).

The limit state exceedance probability is computed using the first order reliability method (FORM) approximation (Der Kiureghian 2005) and considering both the demand and capacity lognormally distributed. The limit state probability of exceedance can be calculated as:

$$P_f = \Phi(-RI) \tag{5}$$

where P_f is the probability of exceedance, calculated for a specified limit state; Φ is the standard normal cumulative distribution function and RI is the reliability index, calculated using the FORM approximation:

$$RI = \frac{\lambda_R - \lambda_S}{\sqrt{\zeta_R^2 + \zeta_S^2}} \tag{6}$$

$$\lambda_R = \ln(\mu_R) - 0.5\zeta^2$$

$$\zeta = \sqrt{\ln(1 + \delta_R^2)}$$

Table 10 Damage scales developed for as-built and retrofitted structures

Limit state (LS)	Drift limit	Roof displacement (mm)			
		As-built models		Retrofitted models	
		Model-3	Model-5	Model-3	Model-5
LS1	Idealized yield	140.00	135.00	100	95
LS2	Code drift limit	180	180	180	180
LS3	Incipient collapse	338	278	350	287

DS1: Damage State 1 (moderate damage) will be achieved by the structures exceeding LS1

DS2: Damage state 2 (heavy damage) will be achieved by the structures exceeding LS2

DS3: Damage state 3 (collapse) will be achieved by the structures exceeding LS3

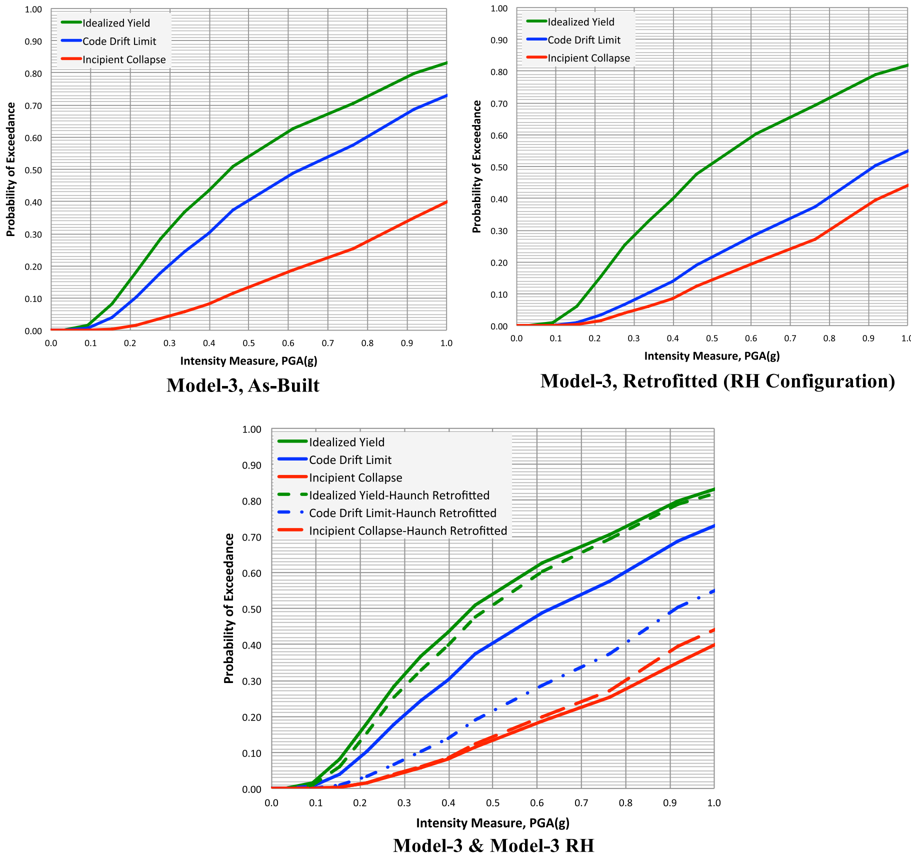

Fig. 19 Fragility functions for Model-3. From top to bottom: as-built (left) and haunch-retrofitted applied below the beam (right), and fragility functions comparison

$$\delta_R = \frac{\sigma_R}{\mu_R}$$

where μ is the mean value, δ is the coefficient of variation, ζ is the logarithmic standard deviation, λ is the median value, the subscript R represents capacity while S represents demand. These parameters will be obtained for both the demand and the capacity to calculate reliability index RI and the limit state exceedance probability P_f using Eq. (5). Similarly, P_f will be calculated for multiple seismic intensity levels for the limit states, which is correlated with the seismic intensity to derive fragility functions. Figures 19 and 20 shows the derived fragility functions for the considered RC frames, as-built and haunch retrofitted.

The fragility functions of both the as-built and retrofitted structures are somewhat comparable for idealized yield limit state damage state but very distinct for code-specified drift limit state. The former is because of the fact that both the as-built and retrofitted structures respond almost similarly in the elastic state but in the inelastic state the as-built RC frames exceed the code-specified drift limit earlier than the retrofitted frames. The later is because of the fact that the haunch retrofitting technique stiffens the beam-column joint and increase the lateral stiffness and strength of structures that consequently retard the damageability of

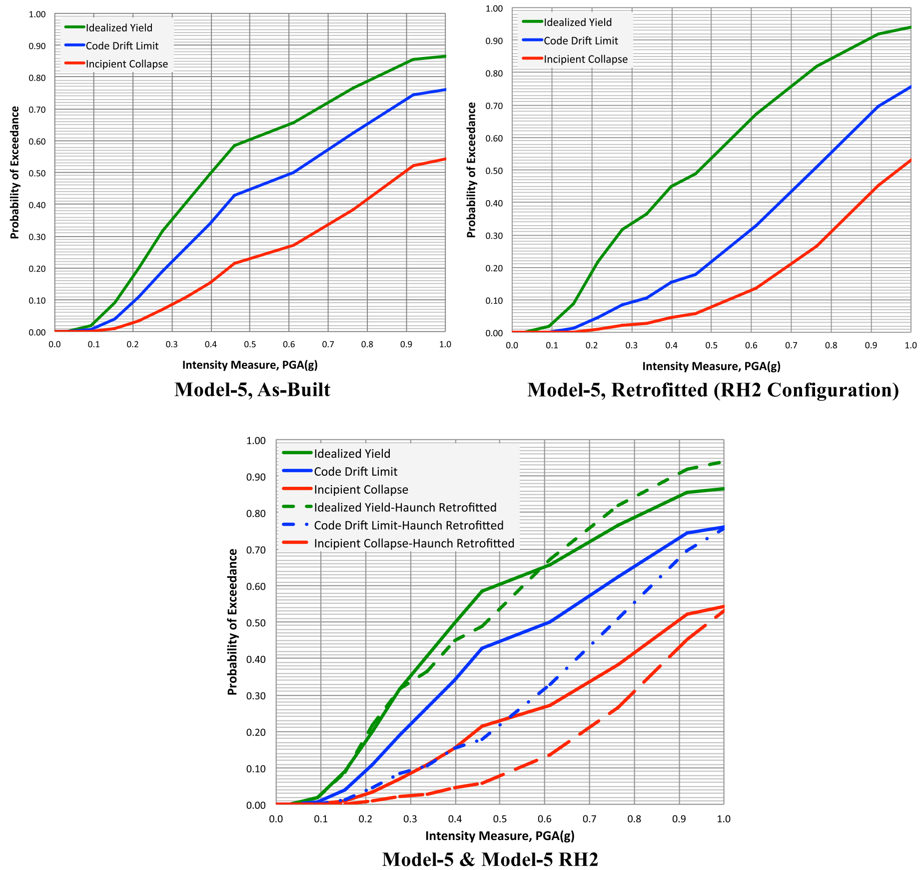

Fig. 20 Fragility functions for Model-5. From top to bottom: as-built (left) and haunch-retrofitted applied below the beam (right), and fragility functions comparison

joint under seismic excitation and reduce the probability of exceedance of code drift limit state. However for Model 3, the probability of exceedance of incipient collapse limit state is also very much similar to the as-built structure. It is due to the fact that onset of cracking in the joint panel zones progress damage rapidly in joint panels in case the haunch is applied only below the beam. In case of Model 5, the application of haunch both below and above the beam retard the joint panel damageability, thereby, reduce the probability of exceedance of code drift limit and incipient collapse limit state, particularly in moderate to high seismic intensity. In case of very high seismic intensity, the limit states probability of exceedance of retrofitted structure becomes comparable to as-built structure, and the benefit of haunch retrofit technique cannot be seen in very high seismic intensity (Fig. 23). It is due to the fact that the haunch primarily stiffen the beam-column connection and shift the plastic hinge from joint shear hinging to beam-column member hinging, however, due to non-seismic design nature of beams and columns this doesn't cause appreciable increase in seismic resistance under very high seismic intensity. Nevertheless, the haunch technique will significantly enhance structure performance under moderate to strong ground shaking.

Fragility functions are extended to derive structures' vulnerability curve, correlating the mean damage ratio (MDR) of structure with the seismic intensity. The MDR is calculated by analyzing the structural fragility functions for a specified level of seismic intensity i.e. a given level of intensity is considered for which the damage statistics are retrieved, analyzing the fragility functions, that quantify the fraction of building stock in a given damage state e.g. pre-yield, post-yield (pre- and post-code drift limit state) and collapse. The structural-damage to monetary-loss model developed by Bal et al. (2008) is used to transform the structural damage statistics to MDR:

$$MDR_i = \sum_{i=1}^{n} \sum_{j=1}^{m} DS_j \times RCR_j \tag{7}$$

where MDR_i is the structure mean damage ratio for a specified seismic intensity level *i, DSj* (*DS1, DS2, DS3*) is the fraction of structure in a given damage state j, calculated from the fragility functions for a specified seismic intensity, RCR_j ($RCR_1 = 0.33$, $RCR_2 = 1.05$, $RCR_3 = 1.04$) is the repair cost ratio (*RCR*) of structure for a specified damage state, defined as per the model of Bal et al. (2008). The derived *MDR* is correlated with the seismic intensity to develop vulnerability curves (Fig. 21). For Model 3, the application of haunch reduce the *MDR* over the whole range of seismic intensity, whereas for Model 5, the haunch application reduce the *MDR* particularly in the range of moderate to high seismic intensity.

5 Cost-benefit analysis of haunch retrofitting

The PBEE time-based assessment procedure is included to assess the performance of the retrofitting technique, quantifying the seismic performance of structures in terms of average annual loss (*AAL*). If calculated for both the as-built and retrofitted structures, the annual avoided expenditure due to retrofitting can be quantified, which is summed over the specified life of structure and converted to net present value that is critically compared with the cost of retrofit to assess its viability:

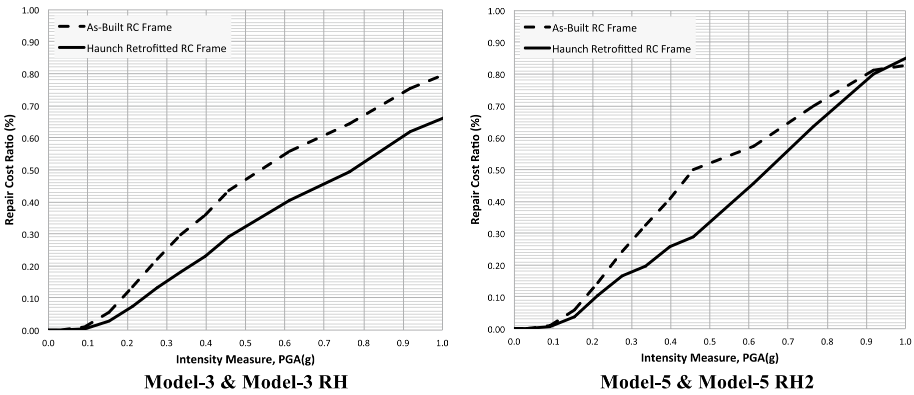

Fig. 21 Vulnerability curves derived for as-built and haunch retrofitted RC frames

$$NPV = A\left\{\frac{1-\frac{1}{(1+i)^t}}{i}\right\} \tag{8}$$

$$A = AAL_{Retrofitted} - AAL_{As-Built}$$

where *NPV* is the net present value of the annual avoided expenditure due to the use of retrofit, *i* is the interest rate (internal rate of return), t is the time span over which the assessment is carried out (equal to intended life of a structure). Given the site seismic hazard, presented in terms of seismic hazard curve specifying the annual probability of exceedance of seismic intensity, and the structure's *MDR* that specify the *RCR* correlated with the seismic intensity, both are related to calculate the *AAL*. For a specified time period (intended life of structure), if the calculated value of *NPV* is larger than the cost of retrofit, there is economic benefit in retrofitting the structure, because the annual avoided cost is greater than the cost of the retrofit.

5.1 Derivation of seismic hazard curve

Two candidate cities are selected to assess probabilistically the benefit of haunch retrofitting scheme for the considered deficient RC frames. The city of Muzaffarabad, which is in the highest seismic zone (Zone 4, as per the BCP-2007) that was once devastated in 2005 Mw 7.6 Kashmir earthquake, and the city of Jhelum, which is in the moderate seismic zone (Zone 2B, as per the BCP-2007) that have experienced moderate to strong earthquakes. Since, the current building code of Pakistan specifies only the design level ground motions for the region. A classical probabilistic seismic hazard analysis (PSHA) technique was adopted, and that including the most up-to-date developments in procedure (Cornell 1968; Reiter 1999; Gutenberg and Richter 1956; McGuire 2004; Abrahamson 2000; Bommer and Stafford 2009; CRISIS 2007), available catalogue (Zare et al. 2014; USGS, ISC, NGDC, Ambraseys and Douglas 2004; Ambraseys 2000; Kale and Akkar 2003; Scherbaum et al. 2009) and seismic sources (PMD 2007; BCP-SP 2007), to obtain ground motions for various return periods and construct seismic hazard curve (Fig. 22).

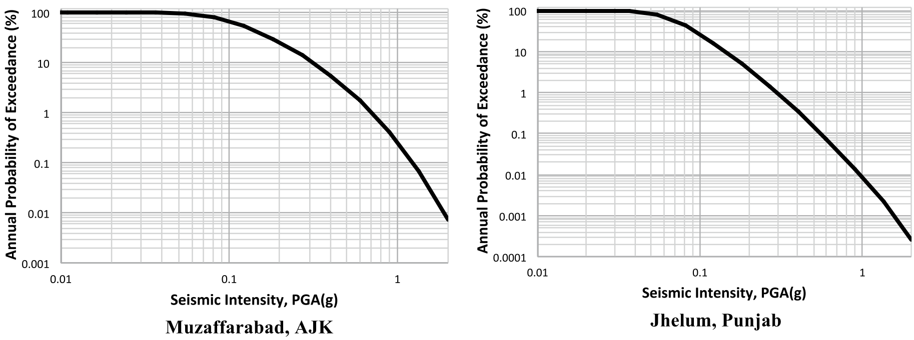

Fig. 22 Uniform seismic hazard curve derived for Muzaffarad (left) and Jhelum (right), using classical PSHA procedure

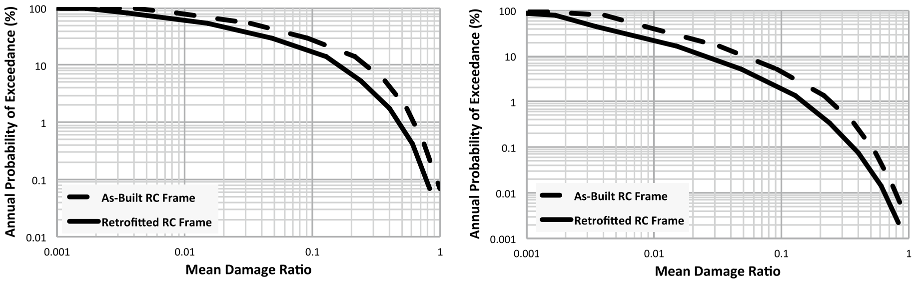

Muzaffarabad, AJK (Zone 4) Jhelum, Punjab (Zone 2B)

Model-3, haunch retrofitted with haunch applied below the beam

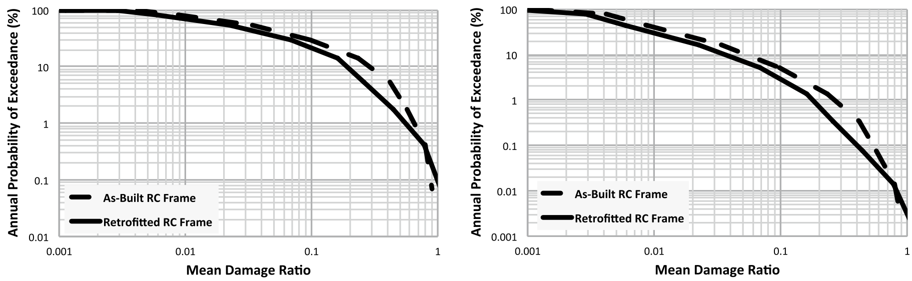

Muzaffarabad, AJK (Zone 4) Jhelum, Punjab (Zone 2B)

Model-5, haunch retrofitted with haunch applied below the beam

Fig. 23 Loss exceedance curves derived for both as-built and haunch retrofitted models for Muzaffarad (left) and Jhelum (right)

5.2 Calculation of average annual loss and cost-benefit analysis

To calculate the *AAL*, for a specified seismic intensity, the *MDR* of structures are retrieved from the vulnerability curve and correlated with the corresponding annual probability of exceedance of seismic intensity, to derive loss exceedance curves (Fig. 23). Haunch retrofitting shift the loss exceedance curve towards the ordinate, which is due to the reduction of mean damage ratio for a specified ground motion, that reduce the area under the loss exceedance curve. For a given structure, the *AAL* is calculated by integrating the loss exceedance curve, using the Simpson's rule and numerical integration to estimate *AAL*:

$$AAL = \sum_{i \to \infty} \left(\frac{APE_{i+1} - APE_i}{6} \right) \times (MDR_i + 4MDR_{i+0.5} + MDR_{i+1}) \tag{9}$$

where *APE* is the annual probability of exceedance of ground motion and *MDR* is the mean damage ratio, $MDR_{i+0.5}$ is approximated as the average of the MDR_{i+1} and MDR_i. Table 11 reports the average annual loss computed for both Model-3 and Model-5 (as-built and haunch retrofitted) in both high and moderate hazard regions i.e. Muzaffarabad, which is Zone 4 (design PGA, 0.40 g on rock site) and Jhelum, which is in Zone 2B (design PGA, 0.20 g on rock site), as per the BCP-SP (2007). The *AAL* computed are incorporated in Eq. (8), to calculate the net present value over the next 50 years. An interest rate of 6% and

Table 11 Average annual loss computed for as-built and haunch retrofitted models over the next 50 years (design life of a structure)

Model	Average annual loss (AAL) Percent of building cost				Net present value (NPV) Percent of building cost		Retrofit cost (percent of building cost)	Cost-benefit ratio (NPV/retrofit cost)	
	As-built		Haunch retrofitted						
	Mzd. (Zone 4)	Jhl. (Zone 2B)	Mzd. (Zone 4)	Jhl. (Zone 2B)	Mzd. (Zone 4)	Jhl. (Zone 2B)		Mzd. (Zone 4)	Jhl. (Zone 2B)
Model-3	10.03	2.58	6.14	1.36	61.44	19.17	5.43	11.32	3.53
Model-5	10.80	2.74	7.67	1.87	49.28	13.70	9.50	5.19	1.44

Model-3 is as built and retrofitted with haunch applied below the beam

Model-5 is as built and retrofitted with haunch applied both above and below the beam

Mzd Muzaffarabad, *Jhl* Jhelum

time span of 50 years are considered. It can be observed that the application of haunch, either applied only below the beam or both above and below the beam, tremendously reduce the average annual loss of the structures.

6 Conclusions

The experimental shake table tests conducted on nine 1:3 reduced scale RC frames (five as-built and four haunch retrofitted) demonstrated that steel haunch applied either only below the beam or both below and above the beam can significantly enhance the seismic performance of deficient RC frames. The haunch retrofit primarily cause increase in the structure stiffness and strength and to some extent in the structural deformability (nevertheless ductility is enhanced). This increase is relatively more in case the haunches are applied both below and above the beam. The retrofitting shifts the initial damages from joint panel zones to beam and column members and retards the joint panel damages, particularly against moderate to strong excitation. The retrofit also enabled the structures to limit the deformation demand under similar imposed excitation.

The FE based modeling technique using SeismoStruct, as proposed earlier for the inelastic modeling of deficient RC frames with joint shear hinging and beam re-bars slip, which was further extended herein for modeling of haunch retrofitted models. It has shown better performance in simulating the roof displacement response of the structures (both as-built and haunch retrofitted) and predicted the peak roof displacement and peak base shear force demand very reasonably; an average error of 5% in peak displacement prediction and less than 3% error in predicting the peak base shear force, this demonstrates the efficiency of the modeling technique and SeismoStruct software.

The seismic fragility functions derived herein revealed that the haunch retrofitting technique largely reduce the probability of exceedance of code-drift limit states under seismic excitations, which indicates that the haunch retrofitting technique is promising in enhancing the seismic performance of structures, particularly under moderate and strong earthquake shaking. Further, the derived vulnerability curves (MDR versus seismic intensity) show a significant reduction in the repair cost ratio of the structure for a specified ground motion. Similarly, the haunch retrofit technique cause a shift in the loss exceedance curve and reduce the area underneath that result in the reduction of the average annual loss (AAL) of the retrofitted structure. The reduced AAL due to retrofitting bring savings in the annual average loss by avoiding a significant portion of the annual losses. This is further demonstrated through the calculation of the net present value of annual avoided loss over the design life of a structures (i.e. 50 years in present case), which was compared with the retrofit cost that resulted in the cost-benefit ratio of larger than 1.0, indicating the economic benefit of the proposed upgradation, demonstrating the economic viability of haunch retrofitting technique for seismic risk mitigation.

Acknowledgements The authors are very grateful to the Editor-in-Chief (Prof. Atilla Ansal) and the Associate Editor (Prof. Andrea Kappos) for generously encouraging the research study. The authors are very grateful to the reviewers for encouraging the research study and providing constructive remarks that further improved quality of the paper. A number of undergraduate and postgraduate students (Shabir Ahmad, Naeem Khan Shinwari, Rifat Ullah, Saud Faisal Farooq, Usama Ali, Arif Ullah, Babar Ilyas) in Department of Civil Engineering of UET Peshawar are highly thanked for their assistance during preparation and testing models. Attaur Rahman is thanked for preparing various drawings.

References

Abrahamson NA (2000) State of the practice of seismic hazard evaluation. In: Proceedings of the GeoEng 2000, Melbourne, Australia
Ahmad N, Ali Q, Crowley H, Pinho R (2014) Earthquake loss estimation of residential buildings in Pakistan. Nat Hazards 73(3):1889–1955
Ahmad N, Shahzad A, Ali Q, Rizwan M, Khan AN (2018) Seismic fragility functions for code compliant and non-compliant RC SMRF structures in Pakistan. Bull Earthq Eng 16(10):4675–4703
Ahmad N, Shahzad A, Rizwan M, Khan AN, Ali SM, Ashraf M, Naseer A, Ali Q, Alam B (2019) Seismic performance assessment of non-compliant SMRF reinforced concrete frame: shake table test study. J Earthq Eng 23(3):444–462
Alath S, Kunnath SK (1995) Modeling inelastic shear deformations in RC beam-column joints. In: Engineering mechanics proceedings of the 10th conference, University of Colorado at Boulder, Boulder, Colorado
Ambraseys N (2000) Reappraisal of north-Indian earthquakes at the turn of the 20th century. Curr Sci 79(9):1237–1250
Ambraseys NN, Douglas J (2004) Magnitude calibration of north Indian earthquakes. Geophys J Int 159(1):165–206
Appa-Rao G, Navya V, Eligehausan R (2013) Strengthening of shear deficient RC beam-column joints in MRFS under seismic loading. In: Proceedings of 8th international conference on fracture mechanics of concrete and concrete structures, Spain
Arslan MH, Korkmaz HH (2007) What is to be learned from damage and failure of reinforced concrete structures during recent earthquakes in Turkey? Eng Fail Anal 14(1):1–22
Ates S, Kahya V, Yurdakul M, Adanur S (2013) Damages on reinforced concrete buildings due to consecutive earthquakes in Van. Soil Dyn Earthq Eng 53:109–118
Aycardi LE, Mander JB, Reinhorn AM (1994) Seismic resistance of reinforced concrete frame structures designed only for gravity loads: experimental performance of subassemblages. ACI Struct J 91(5):552–563
Badrashi YI, Ali Q, Ashraf M (2010) Reinforced concrete buildings in Pakistan—Housing Report. Housing Report No. 159, Earthquake Engineering Research Institute, CA, USA
Bal IE, Crowley H, Pinho R, Gulay G (2008) Detailed assessment of structural characteristics of turkish rc building stock for loss assessment model. Struct Dyn Earthq Eng 28(10–11):914–932
Banazadeh M, Gholhaki M, Sani HP (2017) Cost-benefit analysis of seismic-isolated structures with viscous damper based on loss estimation. Struct Infrastruct Eng 13(8):1045–1055
BCP-SP (2007) Building Code of Pakistan: Seismic Provisions-2007. Ministry of Housing and Works, Islamabad
Benavent-Climent A, Morillas L, Escolano-Margarit D (2014) Seismic performance and damage evaluation of a reinforced concrete frame with hysteretic dampers through shake-table test. Earthq Eng Struct Dyn 43(15):2399–2417
Beres A, Pessiki S, White R, Gergely P (1996) Implications of experiments on the seismic behaviour of gravity load designed rc beam-to-column connections. Earthq Spectra 12(2):185–198
Biddah A, Ghobarah A (1999) Modelling of shear deformation and bond slip in reinforced concrete joints. Struct Eng Mech 7(4):413–432
Bommer JJ, Stafford PJ (2009) Seismic hazard and earthquake actions. In: Elghazouli AY (ed) Seismic design of buildings to Eurocode 8. Spon Press, Oxon, pp 6–46
Bothara JK, Hicyilmas KMO (2008) General observations of building behavior during the 8th October 2005 Pakistan earthquake. Bull N Z Soc Earthq Eng 41(4):209–233
Bracci JM, Reinhorn AM, Mander JB (1995a) Seismic resistance of reinforced concrete frame structures designed for gravity loads. ACI Struct J 92(5):597–609
Bracci J, Reinhorn A, Mander J (1995b) Seismic retrofit of reinforced concrete buildings designed for gravity loads: performance of structural model. ACI Struct J 92(6):711–723
Calvi GM, Magenes G, Pampanin S (2002) Relevance of beam-column joint damage and collapse in RC frame assessment. J Earthq Eng 6(1):75–100
Cardone D, Gesualdi G, Perrone G (2018) Cost-benefit analysis of alternative retrofit strategies for RC frame buildings. J Earthq Eng. https://doi.org/10.1080/13632469.2017.1323041
Celik OC, Ellingwood BR (2008) Modelling beam-column joints in fragility assessment of gravity load designed reinforced concrete frames. J Earthq Eng 12(3):357–381
Chaulagain H, Rodrigues H, Spacone E, Varum H (2015) Seismic response of current RC buildings in Kathmandu Valley. Struct Eng Mech 53(4):791–818
Cornell C (1968) Engineering seismic risk analysis. Bull Seismol Soc Am 58:1583–1606

CRISIS (2007) A software for computing seismic hazard. UNAM, Mexico
Der Kiureghian A (2005) First- and second-order reliability methods. In: Nikolaidis E, Ghiocel DM, Singhal S (eds) Engineering design reliability handbook. CRC Press LLC, Chapter 14
Dolce M, Cardone D, Ponzo FC, Valente C (2005) Shaking table tests on reinforced concrete frames without and with passive control systems. Earthq Eng Struct Dyn 34(14):1687–1717
Dolce M, Cardone D, Ponzo F (2007) Shaking-table tests on reinforced concrete frames with different isolation systems. Earthq Eng Struct Dyn 36:573–596
Doocy S, Daniels A, Packer C, Dick A, Kirsch TD (2013) The human impact of earthquakes: a historical review of events 1980-2009 and systematic literature review. PLoS Curr Disasters. https://doi.org/10.1371/currents.dis.67bd14fe457f1db0b5433a8ee20fb833
Dyanati M, Huang Q, Roke D (2017) Cost-benefit evaluation of self-centering concentrically braced frames considering uncertainties. Struct Infrastruct Eng 13(5):537–553
Engindeniz M, Kahn LF, Zureick AH (2005) Repair and strengthening of reinforced concrete beam-column joints: state of the art. ACI Struct J 102(2):187–197
Erdil B (2016) Why RC buildings failed in the 2011 Van, Turkey, earthquakes: construction versus design practices. J Perform Constr Facil. https://doi.org/10.1061/(asce)cf.1943-5509.0000980
Fintel M (1995) Performance of buildings with shear walls in earthquakes of the last thirty years. PCI J 40(3):62–80
Garcia R, Hajirasouliha I, Pilakoutas K (2010) Seismic behaviour of deficient RC frames strengthened with CFRP composites. Eng Struct 32(10):3075–3085
Genesio G (2012) Seismic assessment of RC exterior beam-column joints and retrofit with haunches using post-installed anchors. PhD Thesis, Stuttgart University, Germany
Ghobarah A, Said A (2001) Seismic rehabilitation of beam-column joints using FRP laminates. J Earthq Eng 5(1):113–129
Gutenberg B, Richter CF (1956) Magnitude and energy of earthquakes. Ann Geofis 9(01):1–15
Hakuto S, Park R, Tanaka H (2000) Seismic load tests on interior and exterior beam-column joints with substandard reinforcing details. ACI Struct J 97(1):11–25
Kale O, Akkar S (2003) A new procedure for selecting and ranking ground-motion prediction equations (GMPEs): the euclidean distance-based ranking (EDR) method. Bull Seismol Soc Am 103(2A):1069–1084
Kim J, LaFave M (2012) A simplified approach to joint shear behavior prediction of RC beam-column connections. Earthq Spectra 28(3):1071–1096
Kuang JS, Wong H (2006) Effects of beam bar anchorage on beam–column joint behavior. Proc Inst Civ Eng Struct Build 159(2):115–124
Kurose Y (1987) Recent studies on reinforced concrete beam-column joints in Japan. PMFSEL Report No. 87-8, Phil M. Ferguson Structural Engineering Laboratory, University of Texas, Austin, Tex, pp 164
Lowes LN, Altoontash A (2003) Modeling reinforced-concrete beam-column joints subjected to cyclic loading. ASCE J Struct Eng 129(12):1686–1697
Marques R, Lamego P, Lourenci PB, Sousa ML (2018) Efficiency and cost-benefit analysis of seismic strengthening techniques for old residential buildings in Lisbon. J Earthq Eng. https://doi.org/10.1080/13632469.2017.1286616
McGuire RK (2004) Seismic hazard and risk analysis. Earthquake Engineering Research Institute (EERI), Oakland, CA, USA
Pampanin S, Calvi GM, Moratti M (2002) Seismic behavior of RC beam-column joints designed for gravity only. In: Proceedings of the 12th European conference on earthquake engineering, Paper No. 726
Pampanin S, Christopoulos C, Chen TH (2006) Development and validation of a metallic haunch seismic retrofit solution for existing under-designed RC frame buildings. Earthq Eng Struct Dyn 35(14):1739–1766
Park R (2002) A summary of results of simulated seismic load tests on reinforced concrete beam-column joints, beams and columns with substandard reinforcing details. J Earthq Eng 6(2):1–27
Pinho R (2007) Nonlinear dynamic analysis of structures subjected to seismic actions. In: Pecker A (ed) Advanced earthquake engineering analysis. Springer, pp 63–89
PMD (2007) Seismic hazard analysis and zonation for Pakistan, Azad Jammu and Kashmir. Technical Report, Pakistan Meteorological Department (PMD), Islamabad, Pakistan
Priestley MJN (1997) Displacement-based seismic assessment of reinforced concrete buildings. J Earthq Eng 1(1):157–192
Priestley MJN, Calvi GM, Kowalsky MJ (2007) Displacement-based seismic design of structures. IUSS Press, Pavia

Quintana-Gallo P, Pampanin S, Carr AJ, Bonelli P (2010) Shake table tests of under designed RC frames for the seismic retrofit of buildings—design and similitude requirements of the benchmark specimen. Proceedings of the New Zealand Society of Earthquake Engineering Paper No. 39
Rashid M, Ahmad N (2017) Economic losses due to earthquake-induced structural damages in RC SMRF structures. Cogent Eng 4(1):1–15
Reiter L (1999) Earthquake hazard analysis. Columbia University Press, New York
Rizwan M, Ahmad N, Khan AN (2018) Seismic performance of SMRF compliant and non-compliant RC frames. ACI Struct J 115(4):1063–1073
Ruiz-Pinilla JG, Adam JM, Perez-Carcel R, Yuste J, Moragues JJ (2016) Learning from RC building structures damaged by the earthquake in Lorca, Spain, in 2011. Eng Fail Anal 68:76–86
Scherbaum F, Delavaud E, Riggelsen C (2009) Model selection in seismic hazard analysis: an information-theoretic perspective. Bull Seismol Soc Am 99(6):3234–3247
SeismoSoft (2016) SeismoSoft—Earthquake Engineering Software Solutions. Available from https://www.seismosoft.com
SeismoMatch (2016) SeismoMatch—Software: a tool for adjusting matching accelerograms to target spectrum using wavelets based appraoch. Available from https://www.seismosoft.com
Sharma A (2013) Seismic behavior and retrofitting of RC frame structures with emphasis on beam-column joints—experiments and numerical modeling. PhD Thesis, Stuttgart University, Germany
Sharma A, Reddy GR, Vaze KK (2011) Shake table tests on a non-seismically detailed RC frame structure. Struct Eng Mech 41(1):1–24
Sharma A, Reddy GR, Eligehausen R, Genesio G, Pampanin S (2014) Seismic response of reinforced concrete frames with haunch retrofit solution. ACI Struct J 111(3):673–684
Shiravand MR, Nejad AK, Bayanifar MH (2017) Seismic response of RC structures rehabilitated with SMA under near-field earthquakes. Struct Eng Mech 63(4):497–507
Sivaselvan M, Reinhorn AM (2001) Hysteretic models for deteriorating inelastic structures. J Eng Mech ASCE 126(6):633–640
Vamvatsikos D, Cornell C (2002) Incremental dynamic analysis. Earthq Eng Struct Dyn 31(3):491–514
Wang B, Zhu S, Xu YL, Jiang H (2017) Seismic retrofitting of non-seismically designed RC beam-column joints using buckling-restrained haunches: design and analysis. J Earthq Eng 1:1. https://doi.org/10.1080/13632469.2016.1277441
Yavari S, Elwood KJ, Wu CL, Lin SH, Hwang SJ, Moehle JP (2013) Shaking table tests on reinforced concrete frames without seismic detailing. ACI Struct J 110(06):1000–1012
Youssef M, Ghobarah A (2001) Modelling of rc beam-column joints and structural walls. J Earthq Eng 5(1):93–111
Zare M, Amini H, Yazdi P, Sesetyan K, Demircioglu MB, Kalafat D, Erdik M, Giardini D, Khan A, Tsereteli N (2014) Recent developments of the Middle East catalog. J Seismolog 18:749–772

Publisher's Note Springer Nature remains neutral with regard to jurisdictional claims in published maps and institutional affiliations.